IET Image Processing

Special issue Call for Papers

Be Seen. Be Cited. Submit your work to a new IET special issue

Connect with researchers and experts in your field and share knowledge.

Be part of the latest research trends, faster.

Read more

IET The Institution of Engineering and Technology

REVIEW

Medical image segmentation using deep learning: A survey

Risheng Wang[1,2] | **Tao Lei[1,2]** | **Ruixia Cui[3]** | **Bingtao Zhang[4]** | **Hongying Meng[5]** | **Asoke K. Nandi[5]**

[1] Shaanxi Joint Laboratory of Artificial Intelligence, Shaanxi University of Science and Technology, Xi'an, China

[2] The School of Electronic Information and Artificial Intelligence, Shaanxi University of Science and Technology, Xi'an, China

[3] The Laboratory of Hepatobiliary Surgery, First Affiliated Hospital' and 'National Engineering Laboratory of Big Data Algorithm and Analysis Technology Research'(Xi'an Jiaotong University), Xi'an, China

[4] The School of Electronic and Information Engineering, Lanzhou Jiaotong University, Lanzhou, China

[5] The Department of Electronic and Electrical Engineering, Brunel University London, UK

Correspondence
Tao Lei, Shaanxi Joint Laboratory of Artificial Intelligence, Shaanxi University of Science and Technology, Xi'an 710021, China.
Email: leitao@sust.edu.cn

Funding information
Natural Science Basic Research Program of Shaanxi, Grant/Award Number: 2021J-47; National Natural Science Foundation of China, Grant/Award Numbers: 61871259, 61861024; Key Research and Development Program of Shaanxi, Grant/Award Number: 2021ZDLGY08-07; Shaanxi Joint Laboratory of Artificial Intelligence, Grant/Award Number: 2020SS-03; National Natural Science Foundation of China-Royal Socie, Grant/Award Numbers: 61811530325, (IECnNSFCn170396 RoyalSociety)

Abstract

Deep learning has been widely used for medical image segmentation and a large number of papers has been presented recording the success of deep learning in the field. A comprehensive thematic survey on medical image segmentation using deep learning techniques is presented. This paper makes two original contributions. Firstly, compared to traditional surveys that directly divide literatures of deep learning on medical image segmentation into many groups and introduce literatures in detail for each group, we classify currently popular literatures according to a multi-level structure from coarse to fine. Secondly, this paper focuses on supervised and weakly supervised learning approaches, without including unsupervised approaches since they have been introduced in many old surveys and they are not popular currently. For supervised learning approaches, we analyse literatures in three aspects: the selection of backbone networks, the design of network blocks, and the improvement of loss functions. For weakly supervised learning approaches, we investigate literature according to data augmentation, transfer learning, and interactive segmentation, separately. Compared to existing surveys, this survey classifies the literatures very differently from before and is more convenient for readers to understand the relevant rationale and will guide them to think of appropriate improvements in medical image segmentation based on deep learning approaches.

1 | INTRODUCTION

Medical image segmentation aims to make anatomical or pathological structures changes in more clear in images; it often plays a key role in computer-aided diagnosis and smart medicine due to the great improvement in diagnostic efficiency and accuracy. Popular medical image segmentation tasks include liver and liver-tumour segmentation [1] [2], brain and brain-tumour segmentation [3] [4], optic disc segmentation [5] [6], cell segmentation [7] [8], lung segmentation, pulmonary nodules [9] [10], and cardiac image segmentation [11] [12]. With the development and popularisation of medical imaging equipments, X-ray, Computed Tomography (CT), Magnetic Resonance Imaging (MRI) and ultrasound have become four important image-assisted means to help clinicians diagnose diseases, to evaluate prognopsis, and to plan operations in medical

institutions. In practical applications, although these ways of imaging have advantages as well as disadvantages, they are useful for the medical examination of different parts of human body.

To help clinicians make accurate diagnosis, it is necessary to segment some crucial objects in medical images and extract features from segmented areas. Early approaches to medical image segmentation often depend on edge detection, template matching techniques, statistical shape models, active contours, machine learning, etc. Zhao et al. [13] proposed a new mathematical morphology edge detection algorithm for lung CT images. Lalonde et al. [14] applied Hausdorff-based template matching to disc inspection, and Chen et al. [15] also employed template matching to perform ventricular segmentation in brain CT images. Tsai et al. [16] proposed a shape-based approach using horizontal sets for 2D segmentation of cardiac MRI images and 3D segmentation of prostate MRI images. Li et al. [17] used the activity profile model to segment liver-tumours from abdominal CT images, while Li et al. [18] proposed a framework for medical body data segmentation by combining level sets and support vector machines (SVMs). Held et al. [19] applied Markov random fields (MRF) to brain MRI image segmentation. Although a large number of approaches have been reported and they are successful in certain circumstances, image segmentation is still one of the most challenging topics in the field of computer vision due to the difficulty of feature representation. In particular, it is more difficult to extract discriminating features from medical images than normal RGB images since the former often suffers from problems of blur, noise, low contrast, etc. Due to the rapid development of deep learning techniques [20], medical image segmentation will no longer require hand-crafted feature and convolutional neural networks (CNN) successfully achieve hierarchical feature representation of images, and thus become the hottest research topic in image processing and computer vision. As CNNs used for feature learning are insensitive to image noise, blur, contrast, etc., they provide excellent segmentation results for medical images.

It is worth mentioning that there are currently two categories of image segmentation tasks, semantic segmentation and instance segmentation. Image semantic segmentation is a pixel-level classification that assigns a corresponding category to each pixel in an image. Compared to semantic segmentation, the instance segmentation not only needs to achieve pixel-level classification, but also needs to distinguish instances on the basis of specific categories. In fact, there are few reports on instance segmentation in medical image segmentation since each organ or tissue is quite different. We review the advances of deep learning techniques on medical image segmentation.

According to the number of labelled data, machine learning is often categorised into supervised learning, weakly supervised learning, and unsupervised learning. The advantage of supervised learning is that we can train models based on carefully labelled data, but it is difficult to obtain a large number of labelled data for medical images. On the contrary, labelled data are not required for unsupervised learning, but the difficulty of learning is increased. Weakly supervised learning is between the supervised and unsupervised learning since it only requires a small part of data labelled while most of data are unlabelled.

Prior to the widespread application of deep learning, researchers had presented many approaches based on model-driven on medical image segmentation. Masood et al. [21] made a comprehensive summary of many model-driven techniques in medical image analysis, including image clustering, region growing, and random forest. In [21], authors summarised different segmentation approaches on medical images according to different mathematical models. Recently, only a few studies based on model-driven techniques were reported, but more and more studies based on data-driven were reported for medical image segmentation. This paper mainly focuses on the evolution and development of deep learning models on medical image segmentation.

In [22], Shen et al. presented a special review of the application of deep learning in medical image analysis. This review summarises the progress of machine learning and deep learning in medical image registration, anatomy and cell structure detection, tissue segmentation, computer-aided disease diagnosis and prognopsis. Litjens et al. [23] reported a survey of deep learning methods, the survey covers the use of deep learning in image classification, object detection, segmentation, registration and other tasks.

More recently, Taghanaki et al. [24] discussed the development of semantic and medical image segmentation; they categorised deep learning-based image segmentation solutions into six groups, that is, deep architectural, data synthesis-based, loss function-based, sequenced models, weakly supervised, and multi-task methods. To develop a more complete survey on medical image segmentation, Seo et al. [25] reviewed classical machine learning algorithms such as Markov random fields, k-means clustering, random forest, and reviewed latest deep learning architectures such as the artificial neural networks (ANNs), the convolutional neural networks (CNNs), and the recurrent neural networks (RNNs). Tajbakhsh et al. [26] reviewed solutions of medical image segmentation with imperfect data sets, including two major data set limitations: scarce annotations and weak annotations. All these surveys play an important role for the development of medical image segmentation techniques. Hesamian et al. [27] reviewed on three aspects of approaches (network structures), training techniques, and challenges. The network structures section describes the main, popular network structures used for image segmentation. The training techniques section discusses the J Digit imaging technique used to train deep neural network models. The challenges section describes the various challenges associated with medical image segmentation using deep learning techniques. Meyer et al. [28] reviewed the advances in the application or potential application of deep learning to radiotherapy. Akkus et al. [29] provided an overview of current deep learning-based segmentation approaches for quantitative brain MRI images. Zhou et al. [30] focused on three typical types of weak supervision: incomplete supervision, inexact supervision and inaccurate supervision. Eelbode et al. [31] focus on evaluating and summarising the optimisation methods used in medical image segmentation tasks based primarily on Dice scores or Jaccard indices.
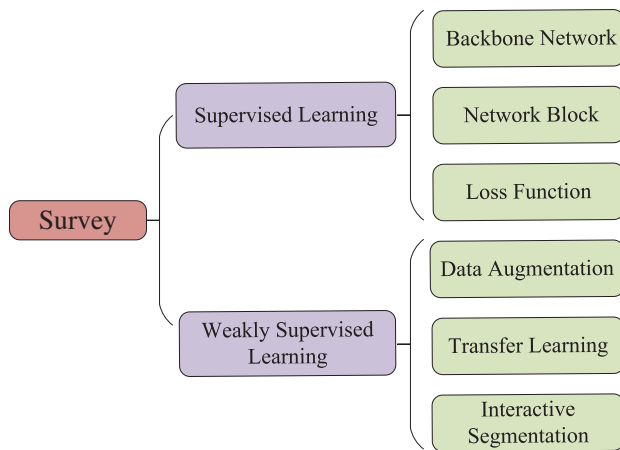
FIGURE 1 An overview of deep learning methods on medical image segmentation

Through studying the aforementioned surveys, researchers can learn the latest techniques of medical image segmentation, and then make more significant contributions for computer-aided diagnoses and smart healthcare. However, these surveys suffer from two problems. One is that most of them chronologically summarise the development of medical image segmentation, and they thus ignore the technical branch of deep learning for medical image segmentation. The other problem is that these surveys only introduce related technical development but not focus on the task characteristics of medical image segmentation such as few-shot learning and imbalance learning, which limits the improvement of medical image segmentation based on task-driven. To address these two problems, we present a novel survey on medical image segmentation using deep learning. In this work, we make the following contributions:

1. We summarise the technical branch of deep learning for medical image segmentation from coarse to fine as shown in Figure 1. The summation includes two aspects of supervised learning and weakly supervised learning. The latest applications of neural architecture search (NAS), graph convolutional networks (GCN), multi-modality data fusion and medical transformer in medical image analysis are also discussed. Compared to the previous surveys, our survey follows conceptual developments and is believed to be clearer.
2. On supervised learning approaches, we analyse literature from three aspects: the selection of backbone networks, the design of network blocks, and the improvement of loss functions. This classification method can help subsequent researchers to understand more deeply motivations and improvement strategies of medical image segmentation networks. For weakly supervised learning, we also review literatures from three aspects for processing few-shot data or class imbalanced data: data augmentation, transfer learning, and interactive segmentation. This organisation is expected to be more conducive to researchers in finding innovations for improving the accuracy of medical image segmentation.

3. In addition to reviewing comprehensively the development and application of deep learning in medical image segmentation, we also collect the currently common public medical image segmentation data sets. Finally, we discuss future research trends and directions in this field.

The rest of this paper is organised as follows. In Section II, we review the development and evolution of supervised learning applied to medical images, including the selection of backbone network, the design of network blocks, and the improvement of loss function. In Section III, we introduce the application of unsupervised or weakly supervised methods in the field of medical image segmentation and analyse the commonly unsupervised or weakly supervised strategies for processing few-shot data or class imbalanced data. In Section IV, we briefly introduce some of the most advanced methods of medical image segmentation, including NAS, application of GCN, and multi-modality data fusion. In Section V, we collect the currently available public medical image segmentation data sets, and summarise limitations of current deep learning methods and future research directions.
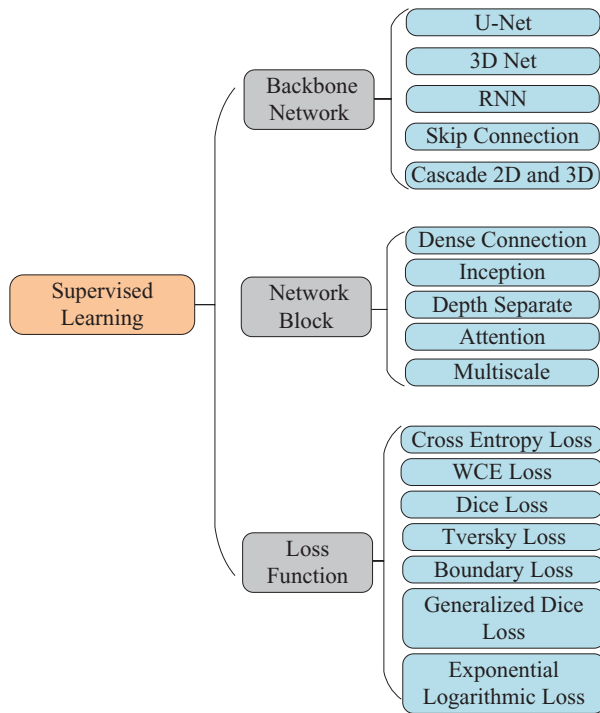
2 | SUPERVISED LEARNING

For medical image segmentation tasks, supervised learning is the most popular method since these tasks usually require high accuracy. In this section, we focus on the review of improvements of neural network architectures. These improvements mainly include network backbones, network blocks and the design of loss functions. Figure 2 shows an overview on the improvement of network architectures based on supervised learning.
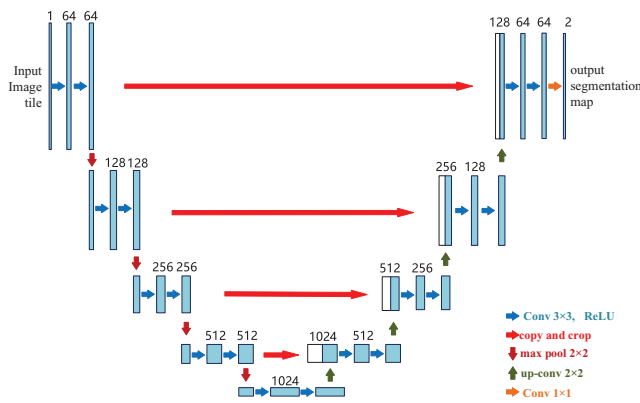
2.1 | Backbone networks

Image semantic segmentation aims to achieve pixel classification of an image. For this goal, researchers proposed the encoder–decoder structure that is one of the most popular end-to-end architectures, such as fully convolution network (FCN) [32], U-Net [7], and Deeplab [33]. In these structures, an encoder is often used to extract image features while a decoder is often used to restore extracted features to the original image size and output the final segmentation results. Although the end-to-end structure is pragmatic for medical image segmentation, it reduces the interpretability of models. The first high-impact encoder–decoder structure, the U-Net proposed by Ronneberger et al. [7], has been widely used for medical image segmentation. Figure 3 shows the U-Net architecture.

U-Net: The U-Net solves problems of general CNN networks used for medical image segmentation, since it adopts a perfect symmetric structure and skip connection. Different from common image segmentation, medical images usually contain noise and show blurred boundaries. Therefore, it is very difficult to detect or recognise objects in medical images only depending on image low-level features. Meanwhile, it is also impossible to
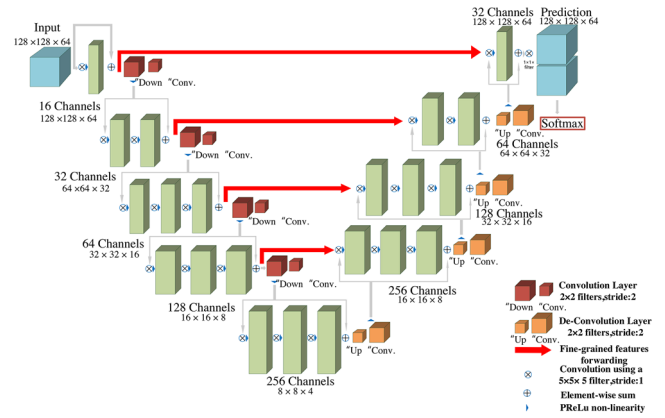
FIGURE 2 An overview of network architectures based on supervised learning

FIGURE 4 The V-Net architecture [35]

FIGURE 5 The recurrent residual convolutional unitalom2018recurrent
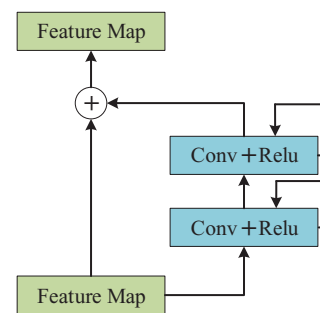

FIGURE 3 The U-Net architecture [7]

obtain accurate boundaries depending only on image semantic features due to the lack of image detail information, whereas the U-Net effectively fuses low-level and high-level image features by combining low-resolution and high-resolution feature maps through skip connections, which is a perfect solution for medical image segmentation tasks. Currently, the U-Net has become the benchmark for most medical image segmentation tasks and has inspired a lot of meaningful improvements.

3D Net: In practice, as most of medical data such as CT and MRI images exist in the form of 3D volume data, the use of 3D convolution kernels can better mine the high-dimensional spatial correlation of data. Motivated by this idea, Çiçek *et al.* [34] extended U-Net architecture to the application of 3D data, and proposed 3D U-Net that deals with 3D medical data directly.

Due to the limitation of computational resources, the 3D U-Net only includes three down-sampling, which cannot effectively extract deep-layer image features leading to limited segmentation accuracy for medical images. In addition, Milletari *et al.* [35] proposed a similar architecture, V-Net, as shown in Figure 4. It is well known that residual connections can avoid vanishing gradient and accelerate network convergence, and it is thus easy to design deeper network structures that can provide better feature representation. Compared to 3D U-Net, V-Net employs residual connections to design a deeper network (four down-samplings), and thus achieves higher performance. Similarly, by applying residual connections to 3D networks, Yu *et al.* [36] presented Voxresnet, Lee *et al.* [37] proposed 3DRUNet, and Xiao *et al.* [38] proposed Res-UNet. However, these 3D Networks encounter same problems of high computational cost and GPU memory usage due to a very large number of parameters.

Recurrent Neural Network (RNN): RNN is initially designed to deal with sequence problems. The long short-term memory (LSTM) network [39] is one of the most popular RNNs. It can retain the gradient flow for a long time by introducing a self-loop. For medical image segmentation, RNN has been used to model the time dependence of image sequences. Alom et al. [40] proposed a medical image segmentation method that combines ResUNet with RNN. The method achieves feature accumulation of recursive residual convolutional layers, which improves feature representation for image segmentation tasks. Figure 5 shows the recurrent residual convolutional unit. Gao

et al. [41] joined LSTM and CNN to model the temporal relationship between different brain MRI slices to improve segmentation accuracy. Bai et al. [42] combined FCN with RNN to mine the spatiotemporal information for aortic sequence segmentation. Clearly, RNN can capture local and global spatial features of images by considering the context information relationship. However, in medical image segmentation, the capture of complete and valid temporal information requires good medical image quality (e.g. smaller slice thickness and pixel spacing). Therefore, the design of RNN is uncommon for improving the performance of medical image segmentation.

Skip Connection: Although the skip connection can fuse low-resolution and high-resolution information and thus improve feature representation, it suffers from the problem of the large semantic gap between low- and high-resolution features, leading to blurred feature maps. To improve skip connection, Ibtehaz et al. [43] proposed MultiResUNet including the Residual Path (ResPath), which makes the encoder features perform some additional convolution operations before fusing with the corresponding features in the decoder. Seo et al. [44] proposed mUNet and Chen et al. [45] proposed FED-Net. Both mU-Net and FED-Net add convolution operations to the skip connection to improve the performance of medical image segmentation.

Cascade of 2D and 3D: For image segmentation tasks, the cascade model often trains two or more models to improve segmentation accuracy. This method is especially popular in medical image segmentation. The cascade model can be broadly divided into three types of frameworks: coarse-fine segmentation, detection segmentation, and mixed segmentation. The first class is a coarse-fine segmentation framework that uses a cascade of two 2D networks for segmentation, where the first network performs coarse segmentation and then uses another network model to achieve fine segmentation based on the previous coarse segmentation results. Christ et al. [46] proposed a cascaded network for liver and liver-tumour segmentation. This network firstly uses an FCN to segment livers, and then uses previous liver segmentation results as the input of the second FCN for liver-tumour segmentation. Yuan et al. [47] first trained a simple convolutional–deconvolutional neural networks (CDNN) model (19-layer FCN) to provide rapid but coarse liver segmentation over the entire images of a CT volume, and then applied another CDNN (29-layer FCN) to the liver region for fine-grained liver segmentation. Finally, the liver segmentation region enhanced by histogram equalisation is considered as an additional input to the third CDNN (29-layer CNN) for liver-tumour segmentation. Besides, other networks using the coarse-fine segmentation framework can be found in [48] [49] [50]. At the same time, the detection segmentation framework is also popular. First, a network model such as R-CNN [51] or You-On-Look-Once (YOLO) [52] is used for target location identification, and then another network is used for further detailed segmentation based on previously coarse segmentation results. Al-Antari et al. [53] proposed a similar approach for breast mass detection, segmentation and classification from mammograms. In this work, the first step is to use the regional deep learning method YOLO for target detection, the second step is to input the detected targets into a newly designed full-resolution convolutional network (FrCN) for segmentation, and finally, a deep convolutional neural network is used to identify the masses and classify them as benign or malignant. Similarly, Tang et al. [47] used faster R-CNN [54] and Deeplab [55] cascades for localisation segmentation of the liver. In addition, both Salehi et al. [56] and Yan et al. [57] proposed a kind of cascade networks for whole-brain MRI and high-resolution mammogram segmentation. This kind of cascade network can effectively extract richer multi-scale context information by using a posteriori probabilities generated by the first network than normal cascade networks.

However, most of medical images are 3D volume data, but a 2D convolutional neural network cannot learn temporal information in the third dimension, and a 3D convolutional neural network often requires high computation cost and serves GPU memory consumption. Therefore some pseudo-3D segmentation methods have been proposed. Oda et al. [58] proposed a three-plane method of cascading three networks to segment the abdominal artery region effectively from the medical CT volume. Vu et al. [59] applied the overlay of adjacent slices as input to the central slice prediction, and then fed the obtained 2D feature map into a standard 2D network for model training. Although these pseudo-3D approaches can segment object from 3D volume data, they only obtain limited accuracy improvement due to the utilisation of local temporal information. Compared to pseudo-3D networks, hybrid cascading 2D and 3D networks are more popular. Li et al. [60] proposed a hybrid densely connected U-Net (H-DenseUNet) for liver and liver-tumour segmentation. This method first employs a simple Resnet to obtain a rough liver segmentation result, utilising the 2D DenseUNet to extract 2D image features effectively, then uses the 3D DenseUNet to extract 3D image features, and finally designs a hybrid feature fusion layer to jointly optimise 2D and 3D features. Although the H-DenseUNet reduces the complexity of models compared to an entire 3D network, the model is complex and it still suffers from a large number of parameters from 3D convolutions. For the problem, Zhang et al. [61] proposed a lightweight hybrid convolutional network (LW-HCN) with a similar structure to the H-DenseUNet, but the former requires fewer parameters and computational cost than the latter due to the design of the depthwise and spatiotemporal separate (DSTS) block and the use of 3D depth separable convolution. Similarly, Dey et al. [62] also designed a cascade of 2D and 3D network for liver and liver-tumour segmentation.

Obviously, among the three types of cascade networks mentioned above, the hybrid 2D and 3D cascade network can effectively improve segmentation accuracy and reduce the learning burdens.

In contrast to the above cascade networks, Valanarasu et al. [63] proposed a complete cascade network namely KiU-Net to perform brain dissection segmentation. The performance of vanilla U-Net is greatly degraded when detecting smaller anatomical structures with fuzzy noise boundaries. To overcome this problem, authors designed a novel over-complete architecture Ki-Net, in which the spatial size of the intermediate layer is larger than that of the input data, and this is achieved by

using an up-sampling layer after each conversion layer in the encoder. Thus the proposed Ki-Net possesses stronger edge capture capability compared to U-Net and finally it is cascaded with the vanilla U-Net to improve the overall segmentation accuracy. Since the KiU-Net can exploit both the low-level fine edges feature maps using Ki-Net and the high-level shape feature maps using U-Net, it not only improves segmentation accuracy but also achieves fast convergence for small anatomical landmarks and blurred noisy boundaries.

Others: A generating adversarial networks (GAN) [64] has been widely used in many areas of computer vision. In its infancy, the GAN was often used for data augmentation by generating new samples, which would be reviewed in Section III, but later researchers discovered that the idea of generative confrontation could be used in almost any field, and was therefore also used for image segmentation. Since medical images usually show low contrast, blurred boundaries between different tissues or between tissues and lesions, and sparse medical image data with labels, U-Net-based segmentation methods using pixel loss to learn local and global relationships between pixels are not sufficient for medical image segmentation, and the use of generative adversarial networks is becoming a popular idea for improving image segmentation. Luc et al. [65] firstly applied the generative adversarial network to image segmentation, where the generative network is used for segmentation models and the adversarial network is trained as a classifier. Singh et al. [66] proposed a conditional generation adversarial network (cGAN) to segment breast tumours within the target area (ROI) in mammograms. The generative network learns to identify tumour regions and generates segmentation results, and the adversarial network learns to distinguish between ground truth and segmentation results from the generative network, thereby enforcing the generative network to obtain labels as realistic as possible. The cGAN works fine when the number of training samples is limited. Conze et al. [67] utilised cascaded pre-trained convolutional encoder–decoders as generators of cGAN for abdominal multi-organ segmentation, and considered the adversarial network as a discriminator to enforces the model to create realistic organ delineations.

In addition, the incorporation of the prior knowledge about organ shape and position may be crucial for improving medical image segmentation effect, where images are corrupted and thus contain artefacts due to limitations of imaging techniques. However, there are few works about how to incorporate prior knowledge into CNN models. As one of the earliest studies in this field, Oktay et al. [68] proposed a novel and general method to combine a priori knowledge of shape and label structure into the anatomically constrained neural networks (ACNN) for medical image analysis tasks. In this way, the neural network training process can be constrained and guided to make more anatomical and meaningful predictions, especially in cases where input image data is not sufficiently informative or consistent enough (e.g. missing object boundaries). Similarly, Boutillon *et al.* [69] incorporated anatomical priors into a conditional adversarial framework for scapula bone segmentation, combining shape priors with conditional neural networks to encourage models to follow global anatomical properties in terms of shape and posi-
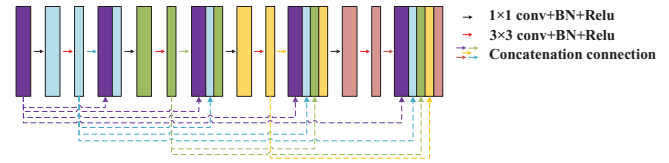

FIGURE 6 Dense connection architecture [70]
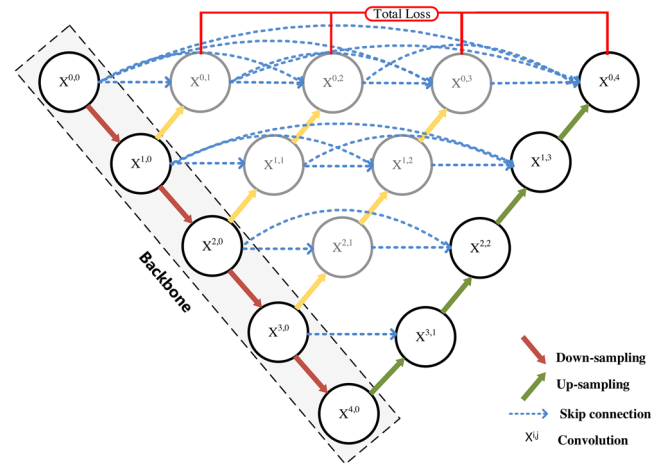

FIGURE 7 The U-Net++ architecture [71]

tion information, and to make segmentation results as accurate as possible. The above study shows that improved models can provide higher segmentation accuracy and they are more robust since prior knowledge constraints are employed in the training process of neural networks.

After proposing U-Net in [7], the encoder–decoder structure became the most popular structure in medical image segmentation. The design of the network backbone focuses on more efficient feature extraction in the encoder and feature recovery and fusion in the decoder to improve segmentation accuracy.

2.2 | Network function block

2.2.1 | Dense connection

Dense connection is often used to construct a kind of special convolution neural networks. For dense connection networks, the input of each layer comes from the output of all previous layers in the process of forward transmission. Inspired by the dense connection, Guan *et al.* [70] proposed an improved U-Net by replacing each sub-block of U-Net with a form of dense connections as shown in Figure 6. Although the dense connection is helpful for obtaining richer image features, it often reduces the robustness of feature representation to a certain extent and increases the number of parameters.

Zhou *et al.* [71] connected all U-Net layers (from one to four) together as shown in Figure 7. The advantage of this structure is that it allows the network to learn automatically
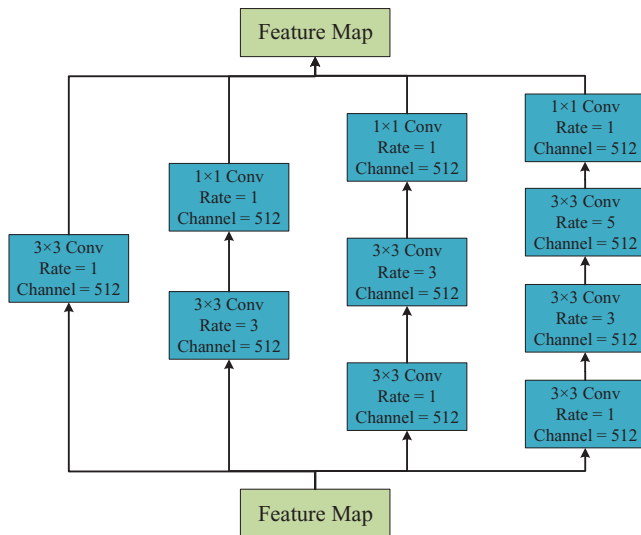
FIGURE 8   The inception architecture [75]. It contains four cascade branches with the gradual increment of the number of atrous convolution, from 1 to 1, 3, and 5, then the receptive field of each branch will be 3, 7, 9, and 19. Therefore, the network can extract features from different scales

importance of features at different layers. Besides, the skip connection is redesigned so that features with different semantic scales can be aggregated in the decoder, resulting in a highly flexible feature fusion scheme. The disadvantage is that the number of parameters is increased due to the employment of dense connection. Therefore, a pruning method is integrated into model optimisation to reduce the number of parameters. Meanwhile, the deep supervision [72] is also employed to balance the decline of segmentation accuracy caused by the pruning. Although the dense connection is helpful for obtaining richer image features, it often reduces the robustness of feature representation to a certain extent and increases the number of parameters.

2.2.2 | Inception

For CNNs, deep networks often give better performances than shallow ones, but they encounter some new problems such as vanishing gradient, the difficulty of network convergence, and the requirement of large memory usage. The inception structure overcomes these problems. It gives better performance by merging convolution kernels in parallel without increasing the depth of networks. This structure is able to extract richer image features using multi-scale convolution kernels, and to perform feature fusion to obtain better feature representation. Inspired by GoogleNet [73] [74], Gu et al. [75] proposed CE-Net by introducing the inception structure into medical image segmentation. The CE-Net adds atrous convolution to each parallel structure to extract features on a wide reception field, and adds 1×1 convolution of feature maps, Figure 8 shows the architecture of the inception. However, the inception structure is complex leading to the difficulty of model modification.

2.2.3 | Depth separability

To improve the generalisation capability of network models and to reduce the requirement of memory usage, many researchers focus on the study of lightweight networks for complex medical 3D volume data. Howard et al. [76] proposed MobileNet to decompose vanilla convolution into depthwise separable convolution and pointwise convolution. The number of vanilla convolution operation is usually $D_K \times D_K \times M \times N$, where M is the dimension of the input feature maps, N is the dimension of the output feature maps, and D_K is the size of the convolution kernels. However, the number of the channel convolution operation is $D_K \times D_K \times 1 \times M$ and the point convolution is $1 \times 1 \times M \times N$. Compared to vanilla convolution, the computational cost of depthwise separable convolution is $(1/N + 1/D_K^2)$ times than that of the vanilla convolution. Based on this, Sandler et al. [77] proposed MobileNet-V2 that contains a novel layer module, the inverted residual with linear bottleneck. In this module, the input is a low-dimensional compressed representation which is first expanded to high dimension and then filtered with a lightweight depthwise convolution. Features are subsequently projected back to a low-dimensional representation with a linear convolution. It allows to significantly reduce the memory footprint needed during inference. By extending the depth separable convolution to the design of 3D networks, Lei et al. [78] proposed a lightweight V-Net (LV-Net) with fewer operations than V-Net for liver segmentation. Besides, Zhang et al. [61] and Huang et al. [79] also proposed the application of depthwise separable convolutions to the segmentation of 3D medical volume data. Other related works for lightweight deep networks can be found in [80] [81]. Depthwise separable convolution is an effective way to reduce the number of model parameters, but it may result in loss of accuracy in medical image segmentation, and thus other approaches (e.g. deep supervision) [78] need to be employed to improve segmentation accuracy.

2.2.4 | Attention mechanism

For neural networks, an attention block can selectively change input or assigns different weights to input variables according to different importance. In recent years, most of researches combining deep learning and visual attention mechanism have focused on using masks to form attention mechanisms. The principle of masks is to design a new layer that can identify key features from an image, through training and learning, and then let networks only focus on interesting areas of images.

Local Spatial Attention: The spatial attention block aims to calculate the feature importance of each pixel in space-domain and extract the key information of an image. Jaderberg et al. [82] early proposed a spatial transformer network (ST-Net) for image classification by using spatial attention that transforms the spatial information of an original image into another space and retains the key information. Normal pooling is equivalent to the information merge that easily causes the loss of key information. For this problem, a block called spatial transformer is
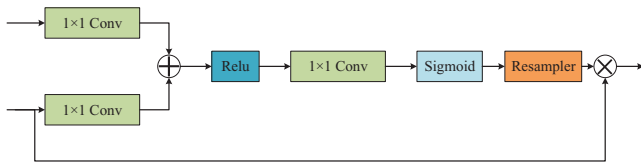
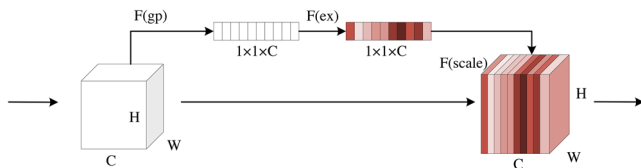**FIGURE 9** The attention block in the attention U-Net [83]

FIGURE 10 The channel attention in the SE-Net [84]

designed to extract key information of images by performing a spatial transformation. Inspired by this, Oktay *et al.* [83] proposed attention U-Net. The improved U-Net uses an attention block to change the output of the encoder before fusing features from the encoder and the corresponding decoder. The attention block outputs a gating signal to control feature importance of pixels at different spatial positions. Figure 9 shows the architecture. This block combines the Relu and sigmoid functions via 1×1 convolution to generate a weight map that is corrected by multiplying features from the encoder.

Channel Attention: The channel attention block can achieve feature recalibration, which utilises learned global information to emphasise selectively useful features and suppress useless features. Hu *et al.* [84] proposed SE-Net that introduced the channel attention to the field of image analysis and won the ImageNet Challenge in 2017. This method implements attention weighting on channels using three steps; Figure 10 shows this architecture. The first is the squeezing operation, the global average pooling is performed on input features to obtain the $1 \times 1 \times Channel$ feature map. The second is the excitation operation, where channel features are interacted to reduce the number of channels, and then the reduced channel features are reconstructed back to the number of channels. Finally, the sigmoid function is employed to generate a feature weight map of $[0, 1]$ that multiplies the scale back to the original input feature. Chen *et al.* [45] proposed FED-Net that uses the SE block to achieve the feature channel attention.

Mixture Attention: Spatial and channel attention mechanisms are two popular strategies for improving feature representation. However, the spatial attention ignores the difference of different channel information and treats each channel equally. On the contrary, the channel attention pools global information directly while ignoring local information in each channel, which is a relatively rough operation. Therefore, combining advantages of two attention mechanisms, researchers have designed many models based on a mixed domain attention block. Kaul *et al.* [85] proposed the focusNet using a mixture of spatial attention and channel attention for medical image segmentation, where the SE-Block is used for channel attention and a branch of spatial

attention is designed. Besides, other related works can be found in [80] [81].

To improve the feature discriminant representation of networks, Wang *et al.* [86] embedded an attention block inside the central bottleneck between the contraction path and the expansion path of the U-Net, and proposed the ScleraSegNet. Furthermore, they compared the performance of channel attention, spatial attention, and different combinations of two attentions for medical image segmentations. They concluded that the channel-centric attention was the most effective in improving image segmentation performance. Based on this conclusion, they finally won the championship of the sclera segmentation benchmarking competition (SSBC2019).

Although those attention mechanisms mentioned above improve the final segmentation performance, they only perform an operation of local convolution. The operation focuses on the area of neighbouring convolution kernels but misses the global information. In addition, the operation of down-sampling leads to the loss of spatial information, which is especially unfavourable for biomedical image segmentation. A basic solution is to extract long-distance information by stacking multiple layers, but this is low efficiency due to a large number of parameters and high computational cost. In the decoder, the up-sampling, the deconvolution, and the interpolation are also performed in the way of local convolution.

Non-local Attention: Recently, Wang *et al.* [87] proposed a non-local U-Net to overcome the drawback of local convolution for medical image segmentation. The non-local U-Net employs the self-attention mechanism and the global aggregation block to extract full image information during the parts of both up-sampling and down-sampling, which can improve the final segmentation accuracy. Figure 11 shows the global aggregation block. The non-local block is a general-purpose block that can be easily embedded in different convolutional neural networks to improve their performance.

It can be seen that the attention mechanism is effective for improving image segmentation accuracy. In fact, spatial attention looks for interesting target regions while channel attention looks for interesting features. The mixed attention mechanism can take advantages of both spaces and channels. However, compared with the nonlocal attention, the conventional attention mechanism lacks the ability of exploiting the associations between different targets and features, so CNNs based on non-local attention usually exhibit better performance than normal CNNs for image segmentation tasks.

2.2.5 | Multi-scale information fusion

One of the challenges in medical image segmentation is a large range of scales among objects. For example, a tumour in the middle or late stage could be much larger than that in the early stage. The size of perceptive field roughly determines how much context information we can use. The general convolution or pooling only employs a single kernel, for instance, a 3×3 kernel for convolution and a 2×2 kernel for pooling.
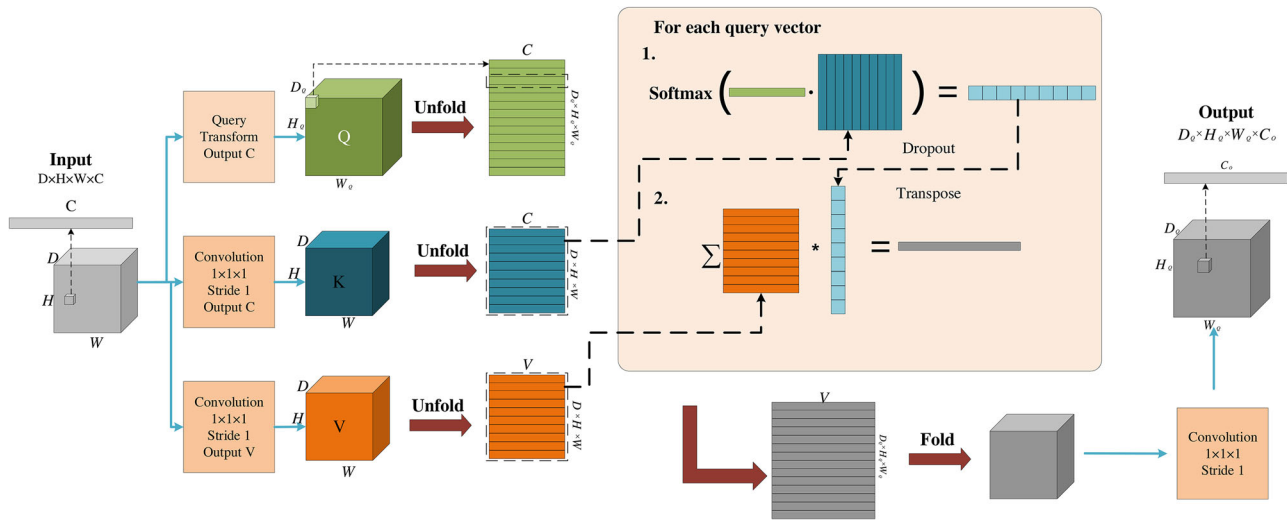
FIGURE 11 The global aggregation block in the non-Local U-Net [87]

Pyramid Pooling: The parallel operation of multi-scale pooling can effectively improve context information of networks, and thus extract richer semantic information. He *et al.* [88] first proposed spatial pyramid pooling (SPP) to achieve multi-scale feature extraction. The SPP divides an image from the fine space to the coarse space, then gathers local features and extracts multi-scale features. Inspired by the SPP, a multi-scale information extraction block is designed and named residual multi-kernel pooling (RMP) [75] that uses four pooling kernels with different sizes to encode global context information. However, the up-sampling operation in RMP cannot restore the loss of detail information due to pooling that usually enlarges the receptive field but reduces the image resolution.

Atrous Spatial Pyramid Pooling: In order to reduce the loss of detail information caused by pooling operation, researchers proposed atrous convolution instead of the polling operation. Compared with the vanilla convolution, the atrous convolution can effectively enlarge the receptive field without increasing the number of parameters. Combining advantages of the atrous convolution and the SPP block, Chen *et al.* [55] proposed the atrous spatial pyramid pooling module (ASPP) to improve image segmentation results. The ASPP shows strong recognition capability on same objects with different scales. Similarly, Similarly, Lopez *et al.* [89] and Lei *et al.* [90] applied superposition of multi-scale atrous convolutions to brain tumour segmentation and liver tumour segmentation, respectively, which achieves a clear accuracy improvement.

However, the ASPP suffers from two serious problems for image segmentation. The first problem is the loss of local information as shown in Figure 12, where we assume that the convolutional kernel is 3×3 and the dilation rate is 2 for three iterations. The second problem is that the information could be irrelevant across large distances. How to simultaneously handle the relationship between objects with different scales is important for designing a fine atrous convolutional network. In response to the above problems, Wang *et al.* [91] designed an hybrid expansion convolution (HDC) networks. This structure
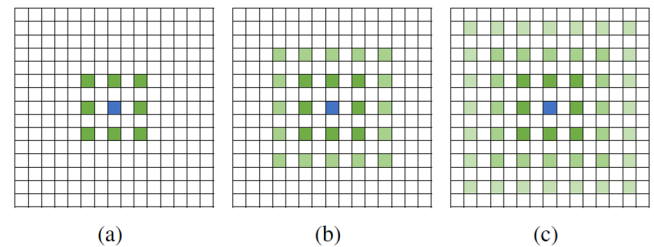

FIGURE 12 The gridding effect (the way of treating images as a chessboard causes the loss of information continuity)

uses a sawtooth wave-like heuristic to allocate the dilation rate, so that information from a wider pixel range can be accessed and thus the gridding effect is suppressed. In [91], authors gave several atrous convolution sequences using variable dilation rate, for example [1,2,3], [3,4,5], [1,2,5], [5,9,17], and [1,2,5,9].

Non-local and ASPP: The atrous convolution can efficiently enlarge the receptive field to collect richer semantic information, but it causes the loss of detail information due to the gridding effect. Therefore, it is necessary to add constraints or establish pixel associations for improving the atrous convolution performance. Recently, Yang *et al.* [92] proposed a combination block of ASPP and non-local for the segmentation of human body parts, as shown in Figure 13. ASPP uses multiple parallel atrous convolutions with different scales to capture richer information, and the non-local operation captures a wide range of dependencies. This combination possesses advantages of both ASPP and non-local, and it has a good application prospect for medical image segmentation.

The network function module is designed to perform more efficient feature fusion. When feature is usually extracted by the encoder, the feature is usually fused by the network function module to enhance the feature representation. Feature fusion is usually performed by fusing different scale information or performing a more efficient way of feature transfer. Then
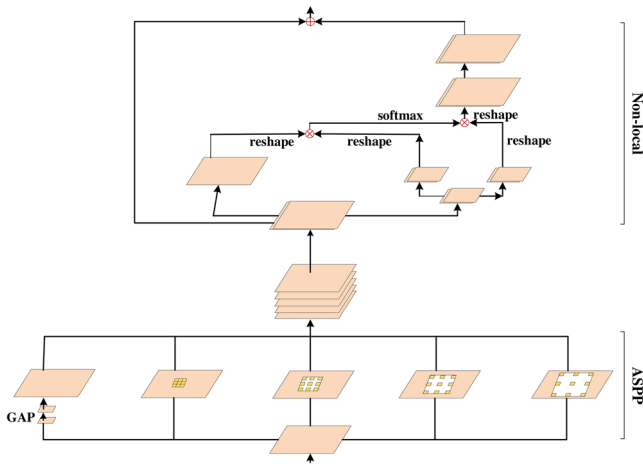
FIGURE 13 The combination of ASPP and non-local architecture [92]

the feature is passed through the decoder to obtain a better segmentation result.

2.3 | Loss function

In addition to improved segmentation speed and accuracy by designing network backbone and the function block, designing new loss functions also resulted in improvements in subsequent inference-time segmentation accuracy. Therefore, a great deal of work has been reported about the design of suitable loss functions for medical image segmentation tasks.

2.3.1 | Cross entropy loss

For image segmentation tasks, the cross-entropy is one of the most popular loss functions. The function compares pixel-wisely the predicted category vector with the real segmentation result vector. For the case of binary segmentation, let $P(Y = 1) = p$ and $P(Y = 0) = 1 - p$, then the prediction is given by the sigmoid function, where $P(\hat{Y} = 1) = 1/(1 + e^{-x}) = \hat{p}$ and $P(\hat{Y} = 0) = 1 - 1/(1 + e^{-x}) = 1 - \hat{p}$, x is the output of neural networks. The cross entropy loss is defined as

$$CE(p, \hat{p}) = -(p\log(\hat{p}) + (1 - p)\log(1 - \hat{p})). \quad (1)$$

2.3.2 | Weighted cross entropy loss

The cross-entropy loss deals with each pixel of images equally, and thus outputs an average value, which ignores the class imbalance and leads to a problem that the loss function depends on the class including the maximal number of pixels. Therefore, the cross-entropy loss often shows low performance for small target segmentation.

To address the problem of class imbalance, Long *et al.* [32] proposed weighted cross-entropy loss (WCE) to counteract the class imbalance. For the case of binary segmentation, the

weighted cross-entropy loss is defined as

$$WCE(p, \hat{p}) = -(\beta p\log(\hat{p}) + (1 - p)\log(1 - \hat{p})), \quad (2)$$

where β is used to tune the proportion of positive and negative samples, and it is an empirical value. If $\beta > 1$, the number of false negatives will be decreased; on the contrary, the number of false positives will be decreased when $\beta < 1$. In fact, the cross-entropy is a special case of the weighted cross-entropy when $\beta = 1$. To adjust the weight of positive and negative samples simultaneously, we can use the balanced cross-entropy (BCE) loss function that is defined as

$$BCE(p, \hat{p}) = -(\beta p\log(\hat{p}) + (1 - \beta)(1 - p)\log(1 - \hat{p})). \quad (3)$$

In [7], Ronneberger *et al.* proposed U-Net in which the cross-entropy loss function is improved by adding a distance function. The improved loss function is able to improve the learning capability of models for inter-class distance. The distance function is defined as

$$D(x) = \omega_0 - e^{\frac{-(d_1(x) + d_2(x))^2}{2\sigma^2}}, \quad (4)$$

where both $d_1(x)$ and $d_2(x)$ denote the distance between the pixel x and boundaries of the first two nearest cells. So the final loss function is defined as

$$L = BCE(p, \hat{p}) + D(x). \quad (5)$$

2.3.3 | Dice loss

The Dice is a popular performance metric for the evaluation of medical image segmentation. This metric is essentially a measure of overlap between a segmentation result and corresponding ground truth. The value of Dice ranges from 0 to 1. '1' means the segmentation result completely overlaps with the real segmentation result. The calculation formula is defined as

$$\text{Dice}(A, B) = \frac{2 \times |A \cap B|}{A + B} \times 100\%, \quad (6)$$

where A is a predicted segmentation result and B is a real segmentation result.

For 3D medical volume data segmentation, Milletari *et al.* [35] proposed V-Net that employs the Dice loss

$$DL(p, \hat{p}) = 1 - \frac{2\langle p, \hat{p} \rangle}{\|p\|_1 + \|p\|_2}, \quad (7)$$

where $\langle p, \hat{p} \rangle$ represents the dot product of the ground truth of each channel and the prediction result matrix.

It is worth noting that the Dice loss is suitable for uneven samples. However, the use of the Dice loss easily influences the back propagation and leads to a training difficulty. Besides, the Dice loss has a low robustness for different models such

as mean surface distance or Hausdorff surface distance due to unbelievable gradient values. For example, the gradient of softmax function can be simplified to $(p-t)$, where t is the target value, and p is the predicted value, but the value of dice loss is $2t^2/(p+t)^2$. If values of p and t are too small, then the gradient value will change drastically leading to training difficulty.

2.3.4 | Tversky loss

Salehi *et al.* [93] proposed the Tversky Loss (TL) that is a regularised version of Dice loss to control the contribution of both false positive and false negative to the loss function. The TL is defined as

$$TL(p, \hat{p}) = \frac{p, \hat{p}}{p, \hat{p} + \beta(1-p, \hat{p}) + (1-\beta)(p, 1-\hat{p})}, \quad (8)$$

where $p \in 0, 1$ and $0 \leq \hat{p} \leq 1$. p and $\hat{p}$ are the ground truth and predicted segmentation, respectively. TL is equivalent to (7) if $\beta = 0.5$.

2.3.5 | Generalised dice loss

Although the Dice loss can solve the problem of class imbalance to a certain extent, it does not work for serious class imbalance. For instance, small targets suffer from prediction errors of some pixels, which easily causes a large change for Dice values. Sudre *et al.* [94] proposed an Generalised Dice Loss (GDL), the GDL is defined as

$$GDL(p, \hat{p}) = 1 - \frac{1}{m} \frac{2 \sum_{j=1}^{m} \omega_j \sum_{i=1}^{n} p_{ij} \hat{p}_{ij}}{\sum_{j=1}^{m} \omega_j \sum_{i=1}^{n} (p_{ij} + \hat{p}_{ij})}, \quad (9)$$

where the weight $\omega = [\omega_1, \omega_2, \dots, \omega_m]$ is assigned to each class, and $\omega_j = 1/(\sum_{i=1}^{n} p_{ij})^2$. The GDL is superior to the Dice loss since different areas have the similar contributions to the loss, and the GDL is more stable and robust during the training process.

2.3.6 | Boundary loss

To solve the problem of class imbalance, Kervadec *et al.* [95] proposed a new boundary loss used for brain lesion segmentation. This loss function aims to minimise the distance between segmented boundaries and labelled boundaries. Authors conducted experiments on two imbalanced data sets with labels. The results show that the combination of the Dice loss and the boundary loss is superior to the single one. The composite loss is defined as

$$L = \alpha L_{GD}(\theta) + (1-\alpha)L_B(\theta), \quad (10)$$

where the first part is a regularised Dice Loss that is defined as

$$L_{GD}(\theta) = 1 - 2(\omega_G \sum_{p \in \Omega} g(p)s_\theta(p)$$
$$+ \omega_B \sum_{p \in \Omega} (1 - g(p))(1 - s_\theta(p)))/$$
$$((\omega_G \sum_{p \in \Omega} [g(p) + s_\theta(p)]$$
$$+ \omega_B \sum_{p \in \Omega} (2 - g(p) - s_\theta(p)))), \quad (11)$$

and the second part is the boundary loss that is defined as

$$L_B(\theta) = \emptyset G(p)s_\theta(p), \quad (12)$$

where if $p \in G$, then $\emptyset G(p) = -||p - z_{\vartheta G}(p)||$, otherwise $\emptyset G(p) = ||p - z_{\vartheta G}(p)||$. Besides, $\sum_\Omega g(p)f(s_\theta(p))$ is used for the foreground and $\sum_\Omega (1 - g(p))(1 - f(s_\theta(p)))$ is used for the background. The $L_{GD}(\theta)$ weight is $\omega_G = 1/(\sum_{p \in \Omega} g(p))^2$ and the $\omega_B = 1/(\sum_{p \in \Omega} (1 - g(p)))^2$. The Ω represents the pixel set in the entire spatial domain.

2.3.7 | Exponential logarithmic loss

In (9), the weighted dice loss is actually that the obtained dice value divides the sum of each label, which achieves a balance for objects with different scales. Therefore, by combining focal loss [96] and dice loss, Wong *et al.* [97] proposed the exponential logarithmic loss (EXP loss) used for brain segmentation to solve problem of serious class imbalance. With the introduction of the exponential form, the non-linearity of the loss functions can be further controlled to improve the segmentation accuracy. The EXP loss function is defined as

$$L_{EXP} = \omega_{\text{dice}} \times L_{\text{dice}} + \omega_{\text{cross}} \times L_{\text{cross}}, \quad (13)$$

where two new parameter weights are denoted by ω_{dice} and ω_{cross}, respectively. The L_{dice} is an exponential log Dice loss, and the L_{cross} is a cross-entropy loss

$$L_{\text{dice}} = E[(-\ln(\text{Dice}_i))^{\gamma_{\text{Dice}}}], \quad (14)$$

$$L_{\text{cross}} = E[\omega_l(-\ln(p_l(x)))^{\gamma_{\text{cross}}}], \quad (15)$$

and,

$$\text{Dice}_i = \frac{2(\sum_x \sigma_{il}(x)p_i(x)) + \varepsilon}{\sum_x (\sigma_{il}(x) + p_i(x)) + \varepsilon}, \quad (16)$$

$$\omega_l = \left(\frac{\sum_k f_k}{f_l} \right)^{0.5}, \qquad (17)$$

where x is pixel position, i is the label and l is the ground-truth value at the position x. The $p_i(x)$ is the probability value outputted from the softmax.

In (17), f_k is the frequency of occurrence of the label k, this parameter can reduce the influence of more frequently seen labels. Both γ_{Dice} and γ_{cross} are used to enhance the non-linearity of the loss function.

2.3.8 | Loss improvements

For medical image segmentation, the improvement of loss mainly focuses on the problem of segmentation of small objects in a large background (the problem of class imbalance). Chen et al. [98] proposed a new loss function by applying traditional active contour energy minimisation to convolutional neural networks, Li *et al.* [99] proposed a new regularisation term to improve the cross-entropy loss function, and Karimi *et al.* [100] proposed a loss function based on Hausdorff distance (HD). Besides, there are still a lot of works [101] [102] trying to deal with this problem by adding penalties to loss functions or changing the optimisation strategy according to specific tasks.

In many medical image segmentation tasks, there are often only one or two targets in an image, and the pixel ratio of targets is sometimes small, which makes network training difficult. Therefore, to improve network training and segmentation accuracy, it is easier to focus on smaller targets by changing loss functions than to change the network structure. However, the design of loss functions is highly task-specific, so we need to analyse carefully task requirement, and then design reasonable and available loss functions.

2.3.9 | Deep supervision

In general, the increase of network depth can improve the feature representation of networks to some extent, but it simultaneously causes new problems such as vanishing gradient and gradient explosion. In order to train deep networks effectively, Lee *et al.* [72] proposed Deeply supervised nets (DSNs) by adding some auxiliary branching classifiers to some layers of the neural network. Dou *et al.* [103] proposed a 3D DSN for heart and liver segmentation, which incorporates a 3D deep monitoring mechanism into a 3D full convolutional network for volume-to-volume learning and inference, eliminating redundant computation and reducing the risk of over-fitting in the case of limited training data. Similarly, Dou *et al.* [104] presented a method for fetal brain MRI cortical plate segmentation using a fully convolutional neural network architecture with deep supervision and residual connection, and obtained high segmentation accuracy for brain MRI cortical plate segmentation. In fact, deep supervision not only constrains the discrimination and robustness of
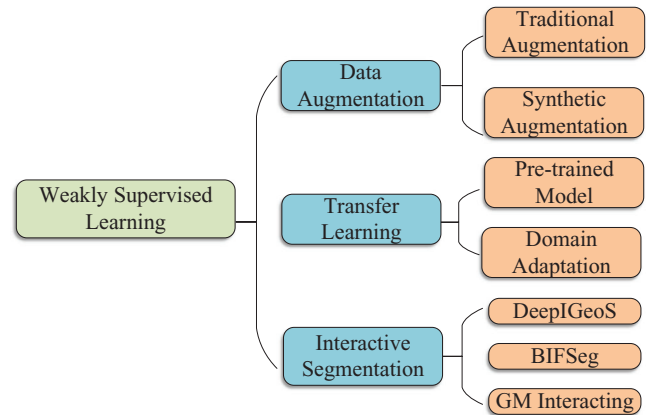
FIGURE 14 The weakly supervised learning methods for medical image segmentation

learned features at all stages, but also improves network training efficiency.

3 | WEAKLY SUPERVISED LEARNING

Although convolutional neural networks show strong adaptability for medical image segmentation, segmentation results seriously depend on high-quality labels. In fact, it is rare to build many data sets with high-quality labels, especially in the field of medical image analysis, since data acquisition and labeling often incur high costs. Therefore, a lot of studies on incomplete or imperfect data sets are reported. We summarise these studies as weakly supervised learning as shown in Figure 14.

3.1 | Data augmentation

In the absence of largely labelled data sets, data augmentation is an effective solution to this problem. However, general data expansion methods produce images that are highly correlated with original images. Compared to common data augmentation approaches, GAN proposed by Goodfellow [64] is currently a popular strategy for data augmentation since GAN overcomes the problem of reliance on original data.

Traditional Methods: General data augmentation methods include the improvement of image quality such as noise suppression, the change of image intensity such as brightness, saturation, and contrast, and the change of image layout such as rotation, distortion, and scaling. Sirinukunwattana et al. [105] utilised the Gaussian blur to achieve data enhancement, which is helpful for performing gland segmentation tasks in the colon tissue images. Dong *et al.* [106] randomly used the brightness enhancement function in 3D MR images to enrich training data for brain tumour segmentation. Contrast enhancement is usually helpful when an image shows uneven intensity. Furthermore, Ronneberger *et al.* [7] used random elastic deformation to perform data expansion on the original data set. In fact, the most commonly method used for traditional data augmentation
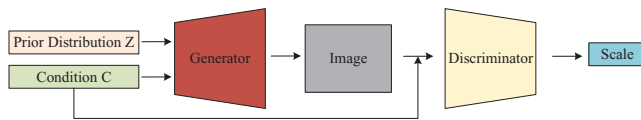
FIGURE 15   The cGAN architecture [108]

FIGURE 16   The Cycle GAN architecture [112]

is parametric transformation (rotation, translation, shear, shift, flip, …). Since this kind of transformation is virtual without computational cost and the annotation on medical images is difficult, it is always performed before each training session.

Conditional Generative Adversarial Nets (cGAN): In contrast to the use of cGAN for supervised learning introduced in Section II, this section focuses on the use of cGAN for data augmentation. An original GAN generator denoted by G can learn data distribution, but generated pictures are random, which means that the generation process of the G is an unguided state. In contrast, cGAN adds a condition to the original GAN in order to guide the generation process of the G. Figure 15 shows the architecture of cGAN. Guibas *et al.* [107] proposed a network architecture composed of a GAN [64] and a cGAN [108]. The random variables are input into the GAN leading to the generation of a synthetic image of fundus blood vessel label, then the generated label map is input into the conditional GAN to generate a real retinal fundi image. Finally, authors verified the authenticity of synthesised images by checking whether the classifier can distinguish a synthesised image from a real image. Mahapatra *et al.* [109] used a cGAN to synthesise X-ray images with required abnormalities, this model considers abnormal X-ray images and lung segmentation labels as inputs, and then generates synthetic X-ray images with same diseases as input X-ray images. At the same time, the segmented label is obtained. In addition, there are also some other works [110] [111] using GAN or cGAN to generate images to achieve data enhancement. Although the image generated by cGAN has many defects, such as blurred boundary and low resolution, the cGAN provides a basic ideas for the later CycleGAN [112] and StarGAN [113] used for the conversion of image styles.

3.2 | Transfer learning

By utilising trained parameters of a model to initialise a new model, transfer learning can achieve fast model training for data with limited labels. One approach is to fine-tune the pre-trained model on ImageNet for the target medical image analysis task, while the other is to migrate the training for data from across domains.

Pre-trained Model: Transfer learning is often used to solve the problem of limited data labelled in medical image analysis, and some researchers found that using pre-trained networks on natural images such as ImageNet as an encoder within a U-Net-like network and then performing fine-tuning on medical data can further improve the segmentation effect of medical images. Kalinin [114] *et al.* considered the VGG-11, VGG-16, and
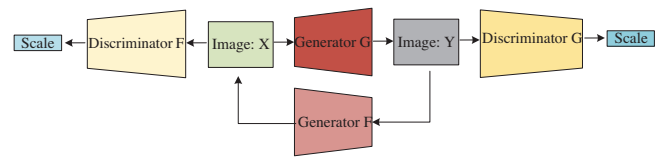
ResNet-34 networks pre-trained on ImageNet as encoders of the U-shaped network to perform semantic segmentation of robotic instruments from wireless capsule endoscopic videos of vascular proliferative lesions and surgical procedures. Similarly, Conze *et al.* [115] used VGG-11 pre-trained on ImageNet as the encoder of a segmentation network to perform shoulder muscle MRI segmentation. Experiments demonstrate that the pre-trained network is useful for improving segmentation accuracy. It can be concluded that a pre-trained model on ImageNet can learn some common underlying features that are required for both medical and natural images, thus retraining process is unnecessary while performing fine-tuning is useful for training models. However, the domain adaptive may be a problem when applying pre-trained models of natural scene images to medical image analysis tasks. Besides, popular transfer learning methods are hardly applicable to 3D medical image analysis because pre-trained models often rely on 2D image data sets. If the number of medical data sets with annotations is large enough, it is possible that the effect of pre-training is weak for improving model performance. In fact, the effect of a pre-trained model is unstable and it depends on segmentation data sets and tasks. Empirically, we can try to use the pre-trained model if it can improve segmentation accuracy, otherwise we need to consider designing new models.

Domain Adaptation: If the labels from the training target domain are not available, and we can only access the labels in other domains, then popular methods are to transfer the trained classifier on the source domain to the target domain without labelled data. CycleGAN is a cycle structure, and mainly composed of two generators and two discriminators. Figure 16 shows the architecture of CycleGAN. First, an image in the X domain is transferred to the Y domain by a generator G, and then the output from the G is reconstructed back to the original image in the X domain by the generator F. On the contrary, the image in the Y domain is transferred to the X domain by the generator F, and then the output from the F is reconstructed back to the original image in the Y domain by the generator G. Both discriminator G and F play discriminating roles ensuring the style transfer of images. Huo *et al.* [116] proposed a jointly optimised image synthesis and segmentation framework for the task of spleen segmentation in CT images using CycleGAN [112]. The framework achieves an image conversion from the marked source domain to the synthesised target domain. During training, synthesised target images are used to train the segmentation network. During the test process, a real image from the target domain is directly input into the trained segmentation network to obtain desired segmentation results. Chen *et al.* [117] also adopted a similar method using

segmentation labels of MR images to achieve the task of cardiac CT segmentation.

Chartsias *et al.* [118] used the CycleGAN to generate corresponding MR images and labels from CT slices and myocardial segmentation labels, and then used synthetic MR and real MR images to train the myocardial segmentation model. This model obtains 15% improvement over the myocardial segmentation model trained on real MR images. Similarly, there are some other works that realise the image conversion between different domains through the CycleGAN and improve the performance of medical image segmentation [119] [120].

3.3 | Interactive segmentation

Manually drawing medical image segmentation labels is usually tedious and time-consuming, especially for the drawing of 3D volume data. Interactive segmentation allows clinicians to correct interactively the initially segmented image generated by a model to obtain more accurate segmentation. The key to effective interactive segmentations is that clinicians can use interactive methods such as mouse clicks and outline boxes to improve an initial segmentation result from a model. Then the model can update parameters and generate new segmentation images to obtain new feedback from the clinicians.

Wang *et al.* [121] proposed the DeepIGeoS using the cascade of two CNNs for interactive segmentation of 2D and 3D medical images. The first CNN called P-Net outputs a coarse segmentation result. Based on this, users provide interactive points or short lines to mark wrong segmentation areas, and then use them as the input of the second CNN called R-Net to obtain corrected results. Experiments were conducted on two-dimensional foetal MRI images and three-dimensional brain tumour images, and experimental results showed that compared with traditional interactive segmentation methods such as Graph-Cuts, RandomWalks and ITK-Snap, the DeepIGeoS greatly reduces the requirement for user interaction and reduces user time.

Wang *et al.* [122] proposed the BIFSeg that is similar to the principle of GrabCut [123] [124]. Users first draw a bounding box, and the area inside the bounding box is considered as the input of CNN, then an initial result is obtained. After that, users perform an image-specific fine-tuning to make CNN provide better segmentation results. The GrabCut achieves image segmentation by learning a Gaussian mixture model (GMM) from images, while the BIFSeg learns a CNN from images. Usually CNN-based segmentation methods can only deal with objects that have appeared in the training set, which limits the flexibility of these methods, but the BIFSeg attempts to use a CNN to segment objects that have not been seen during training process. The process is equivalent to making the BIFSeg learn to extract the foreground part of the object from a bounding box. During the test, the CNN can better use the information in the specific image through an adaptive fine-tuning.

Rupprecht *et al.* [125] proposed a new interactive segmentation method named GM interacting that updates image segmentation results according to the input text from users. This method changes the output of the network by modifying the feature maps between an encoder and a decoder interactively. The category of areas is first set according to the response of users, then some guiding parameters including multiplication and offset coefficients are updated through back propagation, the feature map is finally changed resulting in updated segmentation results.

The interactive image segmentation based on deep learning can reduce the number of user interactions and the user time, which shows broader application prospects.

3.4 | Others works

Semi-supervised learning can use a small part of labelled data and any number of unlabelled data to train a model, and its loss function often consists of the sum of two loss functions. The first is a supervised loss function that is only related with labelled data. The second is an unsupervised loss function or regularisation term that is related to both labelled and unlabelled data.

Based on the idea of GAN, Zhang *et al.* [126] proposed a semi-supervised learning framework based on the adversarial way between segmentation network and evaluation network. An image is fed into U-Net to generate a segmentation map, which is then stacked with the original image and presented to the evaluation network to obtain a segmentation score. During the training process, the segmentation network is optimised in two aspects, one is to minimise the segmentation loss of labelled images and the other is to make the evaluation network obtain high scores for unlabelled images. Besides, the evaluation network is updated to assign low scores to unmarked images but high scores to marked images. Due to this adversarial learning, the segmentation network obtains supervised signals from both labelled and unlabelled images. Thus, the semi-supervised learning framework achieves better segmentation effect in the gland segmentation task for histopathology images. Similarly, some other semi-supervised frameworks [127] [128] [99] [129] are also proposed to optimise medical image segmentation.

Accurate and robust segmentation of organs or lesions from medical images plays a vital role in many clinical applications, such as diagnosis and treatment planning. However, it is difficult for medical images to acquire the annotated data, as generating accurate annotations requires expertise and time. Weakly supervised segmentation methods learn image segmentation from border or image-level labels or from a small amount of annotated image data, rather than using a large number of pixel-level annotations, to obtain high-quality segmentation results. In fact, a small amount of annotated data and a large amount of unannotated data are more compatible with the real clinical situation. However, in practice, the performance of weakly supervised learning only provides rarely acceptable results for medical image segmentation tasks, especially for 3D medical

images. Therefore, this is a direction worth exploring in the future.

4 | CURRENTLY POPULAR DIRECTION

4.1 | Network architecture search

Recently, the performance of convolutional neural network models has been continuously improved. Researchers have designed a large number of popular network architectures for specific tasks such as image classification, segmentation, and reconstruction. These architectures are often designed by industry experts or academics for months or even years, since the design of network architectures with excellent performance usually requires a great deal of domain knowledge. Therefore, the design process is time-consuming and laborious for researchers without domain knowledge. So far, NAS [130] has made significant progress in improving the accuracy of image classification. The NAS can be deemed to a subdomain of automatic machine learning [131](AutoML) and has a strong overlap with hyperparametric optimisation [132] and meta learning [133]. Current research on NAS focuses on three aspects: search space, search strategy and performance estimation. The search space is a candidate collection of network structures to be searched. The search space is divided into a global search space that represents the search for the entire network structure, and a cell-based search space that searches only a few small structures that are assembled into a complete large network by the ways of stacking and stitching. The search strategy aims to find the optimal network structure as fast as possible in search spaces. Popular search strategies are often grouped into three categories: reinforcement-based learning, evolutionary algorithms, and gradients. Performance estimation strategy is the process of assessing how well the network structure performs on target data sets. For NAS techniques, researcher pay more attention to the improvement of search strategies since search space and performance estimation methods are usually rarely changed. Some improved CNN model based on NAS [134] [135] have been proposed and applied to image segmentation.

Most current studies on deep learning in medical image segmentation depend on U-Net networks and makes some changes to the network structure according to different tasks, but in reality the non-network structure factors may be also important for improving segmentation effect. Isensee et al. [136] argued that too much manual adjustment on network structure could lead to over-fitting for a given data set, and therefore proposed a medical image segmentation framework no-new-UNet (nnU-Net) that adapts itself to any new data set. The nnUnet automatically adjusts all hyperparameters according to the properties of the given data set without manual intervention. Therefore, the nnU-Net only relies on vanilla 2D UNet, 3D UNet, UNet cascade and a robust training scheme. It focuses on the stage of pre-processing (resampling and normalisation), training (loss, optimiser settings, data augmentation), inference (e.g. patch-based strategies, test-time-augmentations integra-

tion, model integration), and post-processing (e.g. enhanced single pass domain). In practical applications, the improvements of network structure design usually depend on experiences without adequate interpretability theory support. Moreover, more complex network models indicate higher risk of over-fitting.

Weng et al. [137] first proposed an NAS-UNet for medical image segmentation. The NAS-UNet contains the same two cell architectures DownSC and UpSC. The difference between them is that the former performs a search on the U-shaped backbone to obtain DownSC and UpSC blocks. The NAS-UNet outperforms the U-Net and its variants, and its training time is close to that of U-Net, but with only 6% of the number of parameters.

To perform image segmentation in real time for high-resolution 2D images (e.g. CT, MRI and histopathology images), the study of compressed neural network models has become a popular direction in medical image segmentation. The application of NAS can effectively reduce the number of model parameters and achieves high segmentation performance. Although the performance of NAS is stunning, the fact of why particular architectures perform well cannot be explained. Therefore, it is also important for future research to better understand the mechanisms which have a significant impact on performance and to explore whether these properties can be generalised to different tasks.

4.2 | Graph convolutional neural network

The GCN [138] is one of the powerful tools for the study of non-Euclidean domains. A graph is a data structure consisting of nodes and edges. The early graph neural networks (GNNs) [139] mainly address strictly graphical problems such as the classification of molecular structures. In practice, the Euclidean spaces (e.g. images) or sequences (e.g. text), and many common scenes can be converted into graphs that can be modelled by using GCN techniques.

Gao et al. [140] designed a new graph pooling (gPool) and graph unpooling (gUnpool) operation based on GCN and proposed an encoder–decoder model namely graph U-Net. The graph U-Net achieves better performance than popular U-Nets by adding a small number of parameters. In contrast to traditional convolutional neural networks where deeper is better, the performance of the graph U-Net cannot be improved by increasing the depth of networks when the value of depth exceeds 4. However, the graph U-Net show stronger capability of feature encoding than popular U-Nets when the value of depth is smaller or equivalent to 4. Yang et al. [141] proposed the end-to-end conditional partial residual plot convolutional network CPR-GCN for automatic anatomical marking of coronary arteries. Authors showed that the GCN-based approach provided better performance and stronger robustness than traditional and recent depth learning based approaches. Results from these GCNs in medical image segmentations are promising, as the graph structure has high data representation efficiency and strong capability of feature encoding.

4.3 | Interpretable shape attentive neural network

Currently, many deep learning algorithms tend to make judgments by using 'memorised' models that approximately fit to input data. As a result, these algorithms cannot be explained sufficiently and give convincing evidences for each specific prediction. Therefore, the study of the interpretability of deep neural networks is a hot topic at present.

Sun *et al.* [142] proposed the SAU-Net that focuses on the interpretability and the robustness of models. The proposed architecture attempts to address the problem of poor edge segmentation accuracy in medical images by using a secondary shape stream. Specially, the shape stream and the regular texture stream can capture rich shape-dependent information in parallel. Furthermore, both spatial and channel attention mechanism are used for the decoder to explain the learning capability of models at each resolution of U-Net. Finally, by extracting the learned shape and spatial attention maps, we can interpret the highly activated regions of each decoder block. The learned shape maps can be used to infer correct shapes of interesting categories learned by the model. The SAU-Net is able to learn robust shape features of objects via the gated shape stream, and is also more interpretable than previous works via built-in saliency maps using attention.

Wickstr⊘m *et al.* [143] explored the uncertainty and interpretability of semantic segmentation of colorectal polyps in convolutional neural networks, and the authors developed the central idea of guided back propagation [144] for the interpretation of network gradients. By using back propagation, the gradient corresponding to each pixel in the input is obtained so that the features considered by the network can be visualised. In the process of back propagation, pixels with large and positive gradient values in an image should be paid more attention due to high importance while pixels with large and negative gradient values should be suppressed. If these negative gradients are included in the visualisation of important pixels, they may result in noisy visualisations of descriptive features. To avoid creating noisy visualisations, the guide back propagation process changes the back propagation of the neural network so that the negative gradients are set to zero at each layer, thereby allowing only positive gradients to flow backwards through the network and highlight these pixels.

Medical image analysis is an aid to the clinical diagnosis, the clinicians wonder not only where the lesion is located at, but also the interpretability of results given by networks. Currently, the interpretation of medical image analysis is dominated by visualisation methods such as attention and the class-activation-map (CAM). Therefore, the research on the interpretability of deep learning for medical image segmentation [145] [146] [147] [148] will be a popular direction in future.

4.4 | Multi-modality data fusion

Multi-modality data fusion has been widely used in medical image analysis because it can provide richer object features that are helpful for improving object detection and segmentation results. Dou *et al.* [149] proposed a novel multi-modal learning scheme for accurate segmentation of anatomical structures from unpaired CT and MRI images, and designed a new loss function using knowledge distillation to improve model training efficiency [150]. More specifically, the normalisation layer used for different modalities (i.e. CT and MRI) is implemented within separate variables, whereas the convolutional layer is constructed within shared variables. In each training iteration, samples for each modality are loaded separately and then forwarded to the shared convolutional and independent normalisation layers, and finally the logarithms that can be used to calculate knowledge distillation losses will be obtained. Moeskops *et al.* [151] investigated a question whether it is possible to train a single CNN to perform same segmentation tasks on different-modality data. It is well known that CNNs show excellent performance for image feature encoding and based on this, the experiments in [151] furthermore demonstrate that CNNs are also excellent for feature encoding of multi-modality data when they are used for the same tasks. Therefore, a single system can be used in clinical practice to automatically execute segmentation tasks on various modality data without extra task-specific training.

More relevant literatures can be found in the review on multi-modal fusion for medical image segmentation using deep learning [152]. In this review, authors classified fusion strategies into three categories: input-level fusion, layer-level fusion, and decision-level fusion. Although it is known that multi-modal fusion networks usually show better performance for segmentation tasks than unimodal networks, multi-model fusion causes some new problems such as how to design multi-modal networks to efficiently combine different modalities, how to exploit potential relationships between different modalities, and how to integrate multiple information into segmentation networks to improve segmentation performance. In addition, the integration of multi-modal data fusion into an effective single-parameter network can help simplify deployment and improve the usability of models in clinical practice.

5 | DISCUSSION AND OUTLOOK

5.1 | Medical Image Segmentation Data sets

In order to help clinicians make accurate diagnoses, it is necessary to segment important organs, tissues or lesions from medical images with the aid of a computer and extract features from segmented objects. As a result, various medical image data sets and corresponding competitions have been launched to promote the development of computer-aided diagnosis techniques.
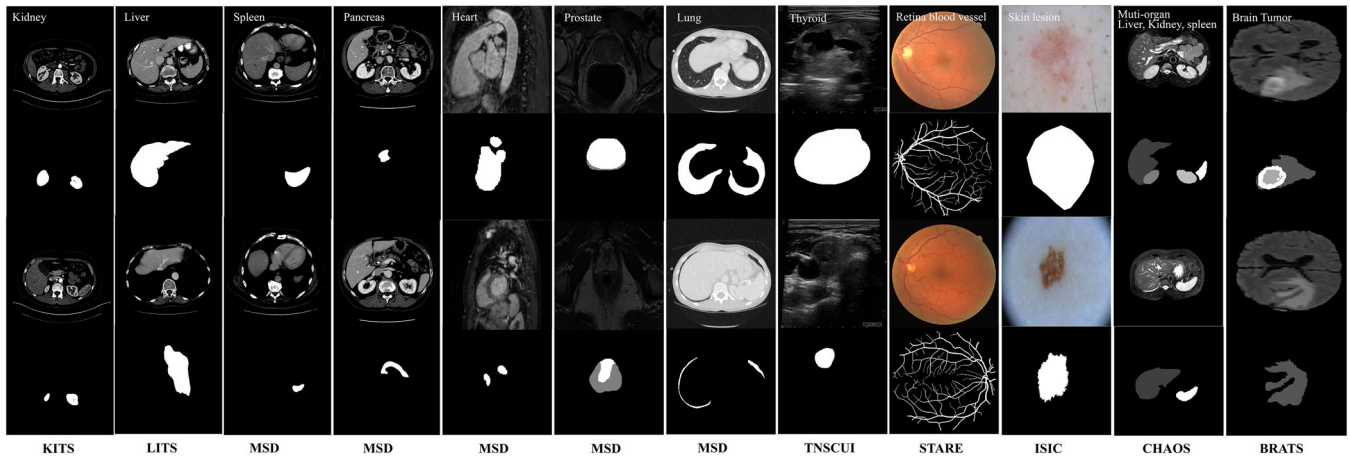
FIGURE 17 Some images of benchmark data sets

In recent years, there has been a growing interest in developing more comprehensive computational anatomical models with the development of deep learning techniques, which has facilitated the development of multi-organ analysis models. The multi-organ segmentation approaches are different from traditional organ-specific strategies in that they incorporate relationships between different organs into models to represent more accurately the complex human anatomy. In the context of multi-organ analysis, brain and abdomen are the most popular in medical image analysis. Thus there are many data sets on the brain and abdomen such as BRATS [3] [153] [154], ISLES [155], KITS [156], LITS [157], and CHAOS [158]. There are two reasons for the emergence of large data sets: on the one hand, the rapid development of imaging techniques, increasingly higher resolution shows more detailed anatomical tissue, which provides a better reference for clinicians; on the other hand, with the development of deep learning techniques, a large number of training samples are necessary, so many research teams have collected many samples and annotated data to form data sets in order to train network models easily. In addition, stable organ structures in the abdomen (e.g. the liver, spleen, and kidneys) can provide constraints and contextual information for creating computational anatomical models of the abdomen. There are also a small number of public data sets on hippocampus and pelvic organs (e.g. Colon [159] and prostate [160]). Indeed, the construction of more holistic and global anatomical models remains one of the greatest challenges and opportunities in future due to the lack of large data sets to characterise the complexity of the human anatomy. More discussions on multi-organ analysis and computational anatomical methods can be found in [161]. The review proposed by Cerrolaza *et al.* [161] follows a methodology-based classification of different techniques that are available for the analysis of multi-organs and multi-anatomical structures, from techniques using point distribution models to the latest deep learning-based approaches.

There are many publicly available data sets for medical image segmentation, Table 1 provides a brief description and list of each data set. As shown in Figure 17, we also provide some images of benchmark data sets. In fact, there are more public data sets than in the list of Table 1 used for medical image segmentation.

5.2 | Popular evaluation metrics

In order to measure effectively the performance of medical image segmentation model, a large number of metrics have been proposed for evaluating the segmentation effectiveness. The evaluation of image segmentation performance relies on pixel quality, region quality and surface distance quality. In this section, we give some popular metrics for evaluating the performance of medical image segmentation. Pixel quality metrics include pixel accuracy (PA). Region quality metrics include Dice score, volume overlap error (VOE) and relative volume difference (RVD). Surface distance quality metrics include average symmetric surface distance (ASD) and maximum symmetric surface distance (MSD).

PA: Pixel accuracy simply finds the ratio of pixels properly classified, divided by the total number of pixels. For $K + 1$ classes (K foreground classes and the background), pixel accuracy is defined as

$$PA = \frac{\sum_{i=0}^{K} p_{ii}}{\sum_{i=0}^{K} \sum_{j=0}^{K} p_{ij}}, \qquad (18)$$

where p_{ij} is the number of pixels of class i predicted as belonging to class j.

Dice score: it is a popular metric for image segmentation (and is more commonly used in medical image analysis), which can be defined as twice the overlap area of predicted and ground-truth maps, divided by the total number of pixels in both images. The Dice score is defined as

$$Dice = \frac{2|A \cap B|}{|A| + |B|}, \qquad (19)$$

TABLE 1 Public data sets for medical segmentation

Objects	Data set	URL
Liver	LiTS [157]	https://competitions.codalab.org/competitions/17094
	Sliver07 [162]	http://www.sliver07.org/
	3Dircadb [163]	https://www.ircad.fr/research/3dircadb/
	Medical Segmentation Decathlon (MSD) [164]	http://medicaldecathlon.com/index.html
	CHAOS [165]	https://chaos.grand-challenge.org
Pancreas	Medical Segmentation Decathlon (MSD) [164]	http://medicaldecathlon.com/index.html
	NIH Pancreas [166]	http://academictorrents.com/details/80ecfefcabede760cdbdf63e38986501f7becd49
Colon	COLONOGRAPHY [159]	https://wiki.cancerimagingarchive.net/display/Public/CT+COLO NOGRAPHY#dc149b9170f54aa29e88f1119e25ba3e
	Medical Segmentation Decathlon (MSD) [164]	http://medicaldecathlon.com/index.html
Heart	AMRG Cardiac Atlas [167]	http://www.cardiacatlas.org/studies/amrg-cardiac-atlas/
	Medical Segmentation Decathlon (MSD) [164]	http://medicaldecathlon.com/index.html
Lung	LIDC-IDRI [168]	https://wiki.cancerimagingarchive.net/display/Public/LIDC-IDRI♯
	VESSEL12 [169]	https://vessel12.grand-challenge.org/
	Medical Segmentation Decathlon (MSD) [164]	http://medicaldecathlon.com/index.html
Prostate	PROMISE12 [160]	https://promise12.grand-challenge.org/
	Medical Segmentation Decathlon (MSD) [164]	http://medicaldecathlon.com/index.html
Brain	OASIS [170]	http://www.oasis-brains.org/
	BRATS [3] [153] [154]	https://www.med.upenn.edu/sbia/brats2018/registration.html
	ISLES [155]	http://www.isles-challenge.org/
	mTOP [171]	https://www.smir.ch/MTOP/Start2016
	Medical Segmentation Decathlon (MSD) [164]	http://medicaldecathlon.com/index.html
Kidney	KITS [156]	https://kits19.grand-challenge.org
	CHAOS [165]	https://chaos.grand-challenge.org
Spleen	Medical Segmentation Decathlon (MSD) [164]	http://medicaldecathlon.com/index.html
	CHAOS [165]	https://chaos.grand-challenge.org
Hippocampus	Medical Segmentation Decathlon (MSD) [164]	http://medicaldecathlon.com/index.html
Hepatic Vessel	Medical Segmentation Decathlon (MSD) [164]	http://medicaldecathlon.com/index.html
Skin lesion	ISIC [172]	https://challenge.isic-archive.com/data
STARE	STARE [173]	https://cecas.clemson.edu/ ahoover/stare/
Thyroid	TNSCUI [174]	https://tn-scui2020.grand-challenge.org/

where A and B denote the ground truth and the predicted segmentation maps, respectively.

VOE: It is the complement of the Jaccard index, it is defined as

$$VOE(A, B) = 1 - \frac{|A \cap B|}{|A \cup B|}. \qquad (20)$$

RVD: It is an asymmetric measure defined as

$$RVD(A, B) = \frac{|B| - |A|}{|A|}. \qquad (21)$$

Surface distance metrics are a set of correlated measures of the distance between the surfaces of a reference and predicted lesion.

Let $S(A)$ denote the set of surface voxels of A. The shortest distance of an arbitrary voxel v to $S(A)$ is defined as

$$d(v, S(A)) = \min_{s_A \in S(A)} (\|v - s_A\|), \qquad (22)$$

where $\| \bullet \|$ denotes the Euclidean distance.

ASD: It is defined as

$$ASD(A, B) = \frac{1}{|S(A)| + |S(B)|} \left(\sum_{s_A \in S(A)} d(s_A, S(B)) \right.$$

$$\left. + \sum_{s_B \in S(B)} d(s_B, S(A)) \right). \qquad (23)$$

MSD: It is also known as the Symmetric Hausdorff Distance, and is similar to *ASD* except that the maximum distance that is taken instead of the average:

$$MSD(A, B) = \max\left\{ \max_{s_A \in S(A)} d(s_A, S(B)), \max_{s_B \in S(B)} d(s_B, S(A)) \right\}. \tag{24}$$

5.3 | Challenges and future scope

It has been proved that fully automated segmentation of medical images based on deep neural networks is very valuable. By reviewing the progress of deep learning in medical image segmentation, we have identified potential difficulties. Researchers successfully employed a variety of means to improve the accuracy of medical image segmentation. Although only the improvement of accuracy cannot account for the performance of algorithms, especially in the field of medical image analysis, where problems of class imbalance, noise interference problems and serious consequences of missed tests must be considered. In the following subsections, we will analyse potential future research directions for medical image segmentation.

5.3.1 | Design of network architecture

In studies of medical image segmentation, the innovation of network structure design is most popular, as the improvement of network structure design shows clear effect and it is easily transferred to other tasks. Through reviewing classical models in recent years, we find that the basic framework of encoder–decoder U-shaped networks with long and short skipped connections has been widely used for medical image segmentation. The residual network (ResNet) and the densely connected network (DenseNet) have demonstrated the effect of deepening network depth and the effectiveness of residual structure on gradient propagation, respectively. Skip connections in deep networks can facilitate gradient propagation and thus reduce the risk of gradient dispersion leading to improved segmentation performance. Furthermore, the optimisation of skipped connections will allow the model to extract richer features.

In addition, the design of the network module is worth exploring. Recently, spatial pyramid modules have been widely used in the field of semantic segmentation. The atrous convolution with fewer parameters allows for wider receptive fields, and the feature pyramid allows for features with different scales to be acquired. The development of spatial channel attention modules makes the process of neural network feature extraction more targeted, so the design of task-specific feature extraction network modules is also well worth investigating.

The manual design of model structures requires rich experiences, so it is inevitable that NAS will gradually replace the manual design. However, it is difficult to search directly a large network due to memory and GPU limitations. Therefore, the future trend should be the combination of manual design and the use of NAS technology. First, a backbone network is designed manually, and then small network modules are searched by NAS before training.

The design of different convolution operations is also a meaningful research direction, such as atrous convolution, deformable convolution, and deep separable convolution. Although these convolutions are all excellent for improving performance of models, they still belong to traditional convolutional categories. As a convolutional method of processing non-Euclidean data, the graph convolution goes beyond the traditional convolution and is valuable for medical data because the graph structure is more efficient and has a strong semantic feature encoding capability.

5.3.2 | Design of loss function

In many medical image segmentation tasks, there are often only one or two targets in an image, and the pixel ratio of targets is sometimes small, which makes network training difficult. For this problem, it is easier to focus on smaller targets by changing loss functions than to change the network structure. However, the design of loss functions is highly task-specific, so we need to analyse carefully task requirement, and then design reasonable and available loss functions.

In specific tasks of medical image segmentation, the use of classical cross-entropy loss functions combined with a specific regularisation term or a specific loss function has become a popular trend. In addition, the use of domain knowledge or a priori knowledge as regular terms or the design of specific loss functions can yield better task-specific segmentation results for medical images. Another avenue is an automatic loss function (or regularisation term) search based on NAS techniques.

5.3.3 | Transfer learning

Medical imaging is usually accompanied by severe noise interference. Moreover, the data annotation of medical images is often more expensive than natural images. Therefore, medical image segmentation based on pre-trained deep learning models on natural images is a worthy direction for future research.

In addition, transfer learning is an important way to achieve weakly supervised medical image segmentation. In fact, transfer learning is the use of existing knowledge to learn new knowledge, and it focuses on finding similarities between existing knowledge and new knowledge. Since most data or tasks are correlated, transfer learning allows us to share the model parameters (or knowledge learned by the model) with the new model in a way that speeds up the efficiency of model learning. Thus, transfer learning can solve the problem of insufficient labelling data.

5.3.4 | Interactive segmentation

Although deep learning has achieved good results in many image segmentation tasks, the vast majority of related works have been with automatic segmentation methods. Many cases still require interactive segmentation methods, such as the annotation of radiotherapy targets, or when user correction is required because the automatic segmentation results are not good enough. In addition, training deep learning models often requires a large number of labelled images as the training data sets that can be done more efficiently with an interactive segmentation tool.

Due to the superior performance of deep learning, the interactive image segmentation [126] based on deep learning can reduce the number of user interactions and the user time that shows broader application prospect.

5.3.5 | Graph convolutional neural network

In general, convolution-based deep neural networks with translation invariance, rotation invariance, scale invariance, shared convolution kernels and fast automatic feature extraction have yielded remarkable results in the field of medical images. However, convolutional neural networks also have many limitations: they rely heavily on geometric priors and it is difficult to capture the intrinsic relationships between different objects using extracted local features, etc. GNN provides a powerful and intuitive modelling approach [175] to the problem of modelling non-Euclidean spaces. Taking the studied objects as nodes and the correlation or similarity between objects as edges, GNN is able to integrate non-Euclidean data and extract invisible relationships between objects by exploiting their intrinsic relationships, and it has been widely used in brain segmentation [176], vessel segmentation [177], prostate segmentation [178], coronary artery segmentation [141], etc.

5.3.6 | Medical transformer

In recent years, deep neural networks based on U-shaped structures and skip connection have been widely used in various medical imaging tasks. However, despite of the fact of achieving excellent performance by CNNs, it is unable to learn global and long-range semantic information interactions well due to the limitations of convolutional operations. Recently, transformer-based architectures have become very popular that replaces the convolutional operator and use self-attention modules to compose entire encoder–decoder structures that can encode long-range dependencies. It has been a great success in the field of natural language processing.

Dosovitskiy *et al.* [179] proposed Vision Transformer (ViT) that is able to classify images directly using the Transformer. Recently, a large number of researches [180] [181] [182] [183] have applied the transformer to medical image segmentation. CNNs have a comparative advantage in extracting the underlying features. These low-level features form the key points, lines, and some basic image structures at the patch level. However, when we detect these basic visual elements, the higher level visual semantic information is often more concerned with how these elements relate to each other to form an object, and how the spatial location of objects relates to each other to form the scene. At present, the transformer is more natural and effective in dealing with the relationships between these elements. However, if all the convolutional operators in CV tasks are replaced by Transformer, it may suffer from many problems, such as high computational cost and memory usage. From existing researches, the combination of Transformer and CNNs may lead to better results.

CONFLICT OF INTEREST
The authors declare no conflict of interest.

DATA AVAILABILITY STATEMENT
The data that support the findings of this study are available from the corresponding author upon reasonable request.

ORCID
Tao Lei https://orcid.org/0000-0002-2104-9298
Hongying Meng https://orcid.org/0000-0002-8836-1382
Asoke K. Nandi https://orcid.org/0000-0001-6248-2875

REFERENCES
1. Li, W.: Automatic segmentation of liver tumor in ct images with deep convolutional neural networks. J. Comput. Commun. 3(11), 146–151 (2015)
2. Vivanti, R., Ephrat, A., Joskowicz, L., Karaaslan, O., Lev Cohain, N., Sosna, J.: Automatic liver tumor segmentation in follow-up CT studies using convolutional neural networks. Sci. Rep. 2, 15497 (2015)
3. Menze, B.H., Jakab, A., Bauer, S., Kalpathy Cramer, J., Farahani, K., Kirby, J., et al.: The multimodal brain tumor image segmentation benchmark (brats). IEEE Trans. Med. Image. 34(10), 1993–2024 (2014)
4. Cherukuri, V., Ssenyonga, P., Warf, B.C., Kulkarni, A.V., Monga, V., Schiff, S.J.: Learning based segmentation of ct brain images: application to post-operative hydrocephalic scans. IEEE Trans. Bio-Med. Eng. 65(8), 1871–1884 (2017)
5. Cheng, J., Liu, J., Xu, Y., Yin, F., Wong, D.W.K., Tan, N.M., et al.: Superpixel classification based optic disc and optic cup segmentation for glaucoma screening. IEEE Trans. Med. Image 32(6), 1019–1032 (2013)
6. Fu, H., Cheng, J., Xu, Y., Wong, D.W.K., Liu, J., Cao, X.: Joint optic disc and cup segmentation based on multi-label deep network and polar transformation. IEEE Trans. Med. Image 37(7), 1597–1605 (2018)
7. Ronneberger, O., Fischer, P., Brox, T.: U-net: Convolutional networks for biomedical image segmentation. Proceedings of the International Conference on Medical Image Computing and Computer-Assisted Intervention (MICCAI), pp. 234–241. (2015)

8. Song, T.H., Sanchez, V., EIDaly, H., Rajpoot, N.M.: Dual-channel active contour model for megakaryocytic cell segmentation in bone marrow trephine histology images. IEEE Trans. Bio-Med. Eng. 64(12), 2913–2923 (2017)

9. Wang, S., Zhou, M., Liu, Z., Liu, Z., Gu, D., Zang, Y., et al.: Central focused convolutional neural networks: developing a data-driven model for lung nodule segmentation. Med. Image Anal. 40, 172–183 (2017)

10. Onishi, Y., Teramoto, A., Tsujimoto, M., Tsukamoto, T., Saito, K., Toyama, H., et al.: Multiplanar analysis for pulmonary nodule classification in CT images using deep convolutional neural network and generative adversarial networks. Int. J. Comput. Assist. Radiol. Surg. 15(1), 173–178 (2020)

11. Wu, F., Zhuang, X.: CF distance: a new domain discrepancy metric and application to explicit domain adaptation for cross-modality cardiac image segmentation. IEEE Trans. Med. Imag. 39(12), 4274–4285 (2020)

12. Chen, C., Qin, C., Qiu, H., Tarroni, G., Duan, J., Bai, W., et al.: Deep learning for cardiac image segmentation: a review. Front. Cardiovas. Med. 7, 25 (2020)

13. Yu Qian, Z., Wei Hua, G., Zhen Cheng, C., Jing Tian, T., Ling Yun, L.: Medical images edge detection based on mathematical morphology. Proc. IEEE Eng. Med. Biol. Soc. 2005, 6492–6495 (2006)

14. Lalonde, M., Beaulieu, M., Gagnon, L.: Fast and robust optic disc detection using pyramidal decomposition and Hausdorff-based template matching. IEEE Trans. Med. Image. 20(11), 1193–1200 (2001)

15. Chen, W., Smith, R., Ji, S.Y., Ward, K.R., Najarian, K.: Automated ventricular systems segmentation in brain CT images by combining low-level segmentation and high-level template matching. BMC Med. Inform. Decis. Mak. 9(S1), S4 (2009)

16. Tsai, A., Yezzi, A., Wells, W., Tempany, C., Tucker, D., Fan, A., et al.: A shape-based approach to the segmentation of medical imagery using level sets. IEEE Trans. Med. Imag. 22(2), 137–154 (2003)

17. Li, C., Wang, X., Eberl, S., Fulham, M., Yin, Y., Chen, J., et al.: A likelihood and local constraint level set model for liver tumor segmentation from CT volumes. IEEE Trans. Biomed. Eng. 60(10), 2967–2977 (2013)

18. Li, S., Fevens, T., Krzyżak, A.: A SVM-based framework for autonomous volumetric medical image segmentation using hierarchical and coupled level sets. Int. Congr. Series. 1268, 207–212 (2004)

19. Held, K., Kops, E.R., Krause, B.J., Wells, W.M., Kikinis, R., Muller Gartner, H.W.: Markov random field segmentation of brain MR images. IEEE Trans. Med. Imaging 16(6), 878–886 (1997)

20. Krizhevsky, A., Sutskever, I., Hinton, G.E.: Imagenet classification with deep convolutional neural networks. Commun. ACM 60(6), 84–90 (2017)

21. Masood, S., Sharif, M., Masood, A., Yasmin, M., Raza, M.: A survey on medical image segmentation. Curr. Med. Imaging Rev. 11(1), 3–14 (2015)

22. Shen, D., Wu, G., Suk, H.I.: Deep learning in medical image analysis. Ann. Rev. Biomed. Eng. 19, 221–248 (2017)

23. Litjens, G., Kooi, T., Bejnordi, B.E., Setio, A.A.A., Ciompi, F., Ghafoorian, M., et al.: A survey on deep learning in medical image analysis. Med. Image Anal. 42, 60–88 (2017)

24. Taghanaki, S.A., Abhishek, K., Cohen, J.P., Cohen.Adad, J., Hamarneh, G.: Deep semantic segmentation of natural and medical images: a review. Artif. Intell. Rev. 54, 137–178 (2021)

25. Seo, H., Badiei Khuzani, M., Vasudevan, V., Huang, C., Ren, H., Xiao, R., et al.: Machine learning techniques for biomedical image segmentation: an overview of technical aspects and introduction to state-of-art applications. Med. Phys. 47(5), e148–e167 (2020)

26. Tajbakhsh, N., Jeyaseelan, L., Li, Q., Chiang, J.N., Wu, Z., Ding, X.: 'Embracing imperfect datasets: a review of deep learning solutions for medical image segmentation. Med. Image Anal. 63, 101693 (2020)

27. Hesamian, M.H., Jia, W., He, X., Kennedy, P.: Deep learning techniques for medical image segmentation: achievements and challenges. J. Digit Imaging 32(4), 582–596 (2019)

28. Meyer, P., Noblet, V., Mazzara, C., Lallement, A.: Survey on deep learning for radiotherapy. Comput. Biol. Med. 98, 126–146 (2018)

29. Akkus, Z., Galimzianova, A., Hoogi, A., Rubin, D.L., Erickson, B.J.: Deep learning for brain MRI segmentation: state of the art and future directions. J. Digit Imaging 30(4), 449–459 (2017)

30. Zhou, Z.H.: A brief introduction to weakly supervised learning. Natl. Sci. Rev. 5(1), 44–53 (2018)

31. Eelbode, T., Bertels, J., Berman, M., Vandermeulen, D., Maes, F., Bisschops, R., et al.: Optimization for medical image segmentation: theory and practice when evaluating with dice score or jaccard index. IEEE Trans. Med. Imaging 39(11), 3679–3690 (2020)

32. Long, J., Shelhamer, E., Darrell, T.: Fully convolutional networks for semantic segmentation. Proceedings of the IEEE Conference on Computer Vision and Pattern Recognition (CVPR), pp. 3431–3440. IEEE, Piscataway, NJ (2015)

33. Chen, L.C., Papandreou, G., Schroff, F., Adam, H.: Rethinking atrous convolution for semantic image segmentation. Preprint, arXiv:170605587 (2017)

34. Çiçek, Ö., Abdulkadir, A., Lienkamp, S.S., Brox, T., Ronneberger, O.: 3d u-net: learning dense volumetric segmentation from sparse annotation. In: Proceedings of the International Conference on Medical Image Computing and Computer-Assisted Intervention (MICCAI), pp. 424–432 (2016)

35. Milletari, F., Navab, N., Ahmadi, S.A.: V-net: fully convolutional neural networks for volumetric medical image segmentation. In: Conference on 3D Vision (3DV), pp. 565–571 (2016)

36. Chen, H., Dou, Q., Yu, L., Heng, P.A.: Voxresnet: deep voxelwise residual networks for volumetric brain segmentation. Preprint, arXiv:160805895 (2016)

37. Lee, K., Zung, J., Li, P., Jain, V., Seung, H.S.: Superhuman accuracy on the snemi3d connectomics challenge. Preprint, arXiv:170600120, (2017)

38. Xiao, X., Lian, S., Luo, Z., Li, S.: Weighted res-unet for high-quality retina vessel segmentation. In: Conference on Information Technology in Medicine and Education (ITME), pp. 327–331 (2018)

39. Hochreiter, S., Schmidhuber, J.: Long short-term memory. Neural Comput. 9(8), 1735–1780 (1997)

40. Alom, M.Z., Hasan, M., Yakopcic, C., Taha, T.M., Asari, V.K.: Recurrent residual convolutional neural network based on u-net (r2u-net) for medical image segmentation. Preprint, arXiv:180206955 (2018)

41. Gao, Y., Phillips, J.M., Zheng, Y., Min, R., Fletcher, P.T., Gerig, G.: Fully convolutional structured LSTM networks for joint 4d medical image segmentation. In: Proceedings of the IEEE International Symposium on Biomedical Imaging (ISBI), pp. 1104–1108. IEEE, Piscataway, NJ (2018)

42. Bai, W., Suzuki, H., Qin, C., Tarroni, G., Oktay, O., Matthews, P.M., et al.: Recurrent neural networks for aortic image sequence segmentation with sparse annotations. In: Proceedings of the International Conference on Medical Image Computing and Computer-Assisted Intervention (MICCAI), pp. 586–594 (2018)

43. Ibtehaz, N., Rahman, M.S.: Multiresunet: rethinking the u-net architecture for multimodal biomedical image segmentation. Neural Netw. 121, 74–87 (2020)

44. Seo, H., Huang, C., Bassenne, M., Xiao, R., Xing, L.: Modified u-net (mu-net) with incorporation of object-dependent high level features for improved liver and liver-tumor segmentation in ct images. IEEE Trans. Med. Imag. 39(5), 1316–1325 (2019)

45. Chen, X., Zhang, R., Yan, P.: Feature fusion encoder decoder network for automatic liver lesion segmentation. In: Proceedings of the IEEE 16th International Symposium on Biomedical Imaging (ISBI), pp. 430–433. IEEE, Piscataway, NJ (2019)

46. Christ, P.F., Elshaer, M.E.A., Ettlinger, F., Tatavarty, S., Bickel, M., Bilic, P., et al.: Automatic liver and lesion segmentation in CT using cascaded fully convolutional neural networks and 3D conditional random fields. In: Proceedings of the International Conference on Medical Image Computing and Computer-Assisted Intervention, pp. 415–423 (2016)

47. Tang, W., Zou, D., Yang, S., Shi, J.: DSL: Automatic liver segmentation with faster R-CNN and DeepLab. In: Proceedings of the International Conference on Artificial Neural Network, pp. 137–147 (2018)

48. Kaluva, K.C., Khened, M., Kori, A., Krishnamurthi, G.: 2D-densely connected convolution neural networks for automatic liver and tumor segmentation'. Preprint, arXiv:180202182 (2018)

49. Feng, X., Wang, C., Cheng, S., Guo, L.: Automatic liver and tumor segmentation of CT based on cascaded U-net. In: Proceedings of the Chinese Intelligent Systems Conference, pp. 155–164 (2019)

50. Albishri, A.A., Shah, S.J.H., Lee, Y.: Cu-net: Cascaded U-net model for automated liver and lesion segmentation and summarization. In: Proceedings of the IEEE International Conference on Bioinformatics and Biomedicine (BIBM), pp. 1416–1423. IEEE, Piscataway, NJ (2019)

51. He, K., Gkioxari, G., Dollár, P., Girshick, R.: Mask R-CNN. Proceedings of the IEEE Conference on Computer Vision (ICCV), pp. 2961–2969. IEEE, Piscataway, NJ (2017)

52. Bochkovskiy, A., Wang, C.Y., Liao, H.Y.M.: Yolov4: optimal speed and accuracy of object detection. Preprint, arXiv:200410934 (2020)

53. Al Antari, M.A., Al Masni, M.A., Choi, M.T., Han, S.M., Kim, T.S.: A fully integrated computer-aided diagnosis system for digital x-ray mammograms via deep learning detection, segmentation, and classification. Int. J. Med. Inform. 117, 44–54 (2018)

54. Ren, S., He, K., Girshick, R., Sun, J.: Faster R-CNN: Towards real-time object detection with region proposal networks. IEEE Trans. Pattern Anal. Mach. Intell. 39(6), 1137–1149 (2016)

55. Chen, L.C., Papandreou, G., Kokkinos, I., Murphy, K., Yuille, A.L.: Deeplab: semantic image segmentation with deep convolutional nets, atrous convolution, and fully connected CRFS. IEEE Trans. Pattern Anal. Mach. Intell. 40(4), 834–848 (2017)

56. Salehi, S.S.M., Erdogmus, D., Gholipour, A.: Auto-context convolutional neural network (auto-net) for brain extraction in magnetic resonance imaging. IEEE Trans. Med. Imaging 36(11), 2319–2330 (2017)

57. Yan, Y., Conze, P.H., Decencière, E., Lamard, M., Quellec, G., Cochener, B., et al.: Cascaded multi-scale convolutional encoder-decoders for breast mass segmentation in high-resolution mammograms. Annual International Conference of the IEEE Engineering in Medicine and Biology Society (EMBC). pp. 6738–6741 (2019)

58. Oda, M., Roth, H.R., Kitasaka, T., Misawa, K., Fujiwara, M., Mori, K.: Abdominal artery segmentation method from CT volumes using fully convolutional neural network. Int. J. Comput. Assist. Radiol. Surg. 14(12), 2069–2081 (2019)

59. Vu, M.H., Grimbergen, G., Nyholm, T., Löfstedt, T.: Evaluation of multi-slice inputs to convolutional neural networks for medical image segmentation. Preprint, arXiv:191209287 (2019)

60. Li, X., Chen, H., Qi, X., Dou, Q., Fu, C.W., Heng, P.A.: H-denseunet: hybrid densely connected UNet for liver and tumor segmentation from ct volumes. IEEE Trans. Med. Imag. 37(12), 2663–2674 (2018)

61. Zhang, J., Xie, Y., Zhang, P., Chen, H., Xia, Y., Shen, C.: Light-weight hybrid convolutional network for liver tumor segmentation. Int. Joint Conf. Artif. Intell. (IJCAI), pp. 4271–4277 (2019)

62. Dey, R., Hong, Y.: Hybrid cascaded neural network for liver lesion segmentation. In: Proceedings of the IEEE International Symposium on Biomedical Imaging (ISBI), pp. 1173–1177. IEEE, Piscataway, NJ (2020)

63. Valanarasu, J.M.J., Sindagi, V.A., Hacihaliloglu, I., Patel, V.M.: Kiu-net: towards accurate segmentation of biomedical images using over-complete representations. In: Proceedings of the International Conference on Medical Image Computing and Computer-Assisted Intervention (MICCAI), pp. 363–373 (2020)

64. Goodfellow, I., Pouget Abadie, J., Mirza, M., Xu, B., Warde Farley, D., Ozair, S., et al.: Generative adversarial nets. Adv. Neural. Inform. Process Syst. 27, 2672–2680 (2014)

65. Luc, P., Couprie, C., Chintala, S., Verbeek, J.: Semantic segmentation using adversarial networks. Preprint, arXiv:161108408 (2016)

66. Singh, V.K., Rashwan, H.A., Romani, S., Akram, F., Pandey, N., Sarker, M.M.K., et al.: Breast tumor segmentation and shape classification in mammograms using generative adversarial and convolutional neural network. Expert Syst. Appl. 139, 112855 (2020)

67. Conze, P.H., Kavur, A.E., Gall, E.C.L., Gezer, N.S., Meur, Y.L., Selver, M.A., Conze Pierre-Henri, Kavur Ali Emre, Cornec-Le Gall Emilie, Gezer Naciye Sinem, Le Meur Yannick, Selver M. Alper, Rousseau François: Abdominal multi-organ segmentation with cascaded convolutional and adversarial deep networks. Artif. Intell. Med. 117, 102109 (2021)

68. Oktay, O., Ferrante, E., Kamnitsas, K., Heinrich, M., Bai, W., Caballero, J., et al.: Anatomically constrained neural networks (ACNNS): application to cardiac image enhancement and segmentation. IEEE Trans. Med. Image 37(2), 384–395 (2017)

69. Boutillon, A., Borotikar, B., Burdin, V., Conze, P.H.: Combining shape priors with conditional adversarial networks for improved scapula segmentation in mr images. In: Proceedings of the IEEE International Symposium on Biomedical Imaging (ISBI), 1164–1167 (2020)

70. Guan, S., Khan, A.A., Sikdar, S., Chitnis, P.V.: Fully dense unet for 2-d sparse photoacoustic tomography artifact removal. IEEE J. Biomed. Health Informat. 24(2), 568–576 (2019)

71. Zhou, Z., Siddiquee, M.M.R., Tajbakhsh, N., Liang, J.: Unet++: redesigning skip connections to exploit multiscale features in image segmentation, IEEE Trans. Med. Imag. 39(6), 1856–1867 (2019)

72. Lee, C.Y., Xie, S., Gallagher, P., Zhang, Z., Tu, Z.: Deeply-supervised nets. Artif. Intell. Statist. 38, 562–570 (2015)

73. Szegedy, C., Liu, W., Jia, Y., Sermanet, P., Reed, S., Anguelov, D., et al.: Going deeper with convolutions. In: Proceedings of the IEEE Conference on Computer Vision and Pattern Recognition (CVPR), pp. 1–9. IEEE, Piscataway, NJ (2015)

74. Szegedy, C., Vanhoucke, V., Ioffe, S., Shlens, J., Wojna, Z.: Rethinking the inception architecture for computer vision. In: Proceedings of the IEEE Conference on Computer Vision and Pattern Recognition (CVPR), pp. 2818–2826. IEEE, Piscataway, NJ (2016)

75. Gu, Z., Cheng, J., Fu, H., Zhou, K., Hao, H., Zhao, Y., et al.: Ce-net: context encoder network for 2D medical image segmentation. IEEE Trans. Med. Imag. 38(10), 2281–2292 (2019)

76. Howard, A.G., Zhu, M., Chen, B., Kalenichenko, D., Wang, W., Weyand, T., et al.: Mobilenets: efficient convolutional neural networks for mobile vision applications. Preprint, arXiv:170404861 (2017)

77. Sandler, M., Howard, A., Zhu, M., Zhmoginov, A., Chen, L.C.: Mobilenetv2: Inverted residuals and linear bottlenecks. In: Proceedings of the IEEE Conference on Computer Vision and Pattern Recognition, pp. 4510–4520. IEEE, Piscataway, NJ (2018)

78. Lei, T., Zhou, W., Zhang, Y., Wang, R., Meng, H., Nandi, A.K.: Lightweight V-net for liver segmentation. In: IEEE International Conference on Acoustic Speech and Signal Processing (ICASSP), pp. 1379–1383. IEEE, Piscataway, NJ (2020)

79. Huang, C., Han, H., Yao, Q., Zhu, S., Zhou, S.K.: 3D U net: A 3D universal U-net for multi-domain medical image segmentation. In: Proceedings of the International Conference on Medical Image Computing and Computer-Assisted Intervention (MICCAI), pp. 291–299 (2019)

80. Paschali, M., Gasperini, S., Roy, A.G., Fang, M.Y.S., Navab, N.: 3DQ: compact quantized neural networks for volumetric whole brain segmentation. In: Proceedings of the International Conference on Medical Image Computing and Computer-Assisted Intervention (MICCAI), pp. 438-446 (2019)

81. Xu, X., Lu, Q., Yang, L., Hu, S., Chen, D., Hu, Y., et al.: Quantization of fully convolutional networks for accurate biomedical image segmentation. In: Proceedings of the IEEE Conference on Computer Vision and Pattern Recognition (CVPR), pp. 8300–8308. IEEE, Piscataway, NJ (2018)

82. Jaderberg, M., Simonyan, K., Zisserman, A., et al.: Spatial transformer networks. In: Proceedings of the Advances in Neural Information Process Systems, pp. 2017–2025 (2015)

83. Oktay, O., Schlemper, J., Folgoc, L.L., Lee, M., Heinrich, M., Misawa, K. et al.: Attention u-net: learning where to look for the pancreas. Preprint, arXiv:180403999 (2018)

84. Hu, J., Shen, L., Sun, G.: Squeeze-and-excitation networks. In: Proceedings of the IEEE Conference on Computer Vision and Pattern Recognition, pp. 7132–7141. IEEE, Piscataway, NJ (2018)

85. Kaul, C., Manandhar, S., Pears, N.: Focusnet: an attention-based fully convolutional network for medical image segmentation. In: Proceedings of the IEEE 16th International Symposium on Biomedical Imaging (ISBI), pp. 455–458. IEEE, Piscataway, NJ (2019)

86. Wang, C., He, Y., Liu, Y., He, Z., He, R., Sun, Z.: Sclerasegnet: an improved u-net model with attention for accurate sclera segmentation.

Proceedings of the IAPR International Conference on Biometrics, pp. 1–8 (2019)

87. Wang, Z., Zou, N., Shen, D., Ji, S.: Non-local u-nets for biomedical image segmentation. In: Proceedings of the AAAI Conference on Artificial Intelligence, pp. 6315–6322 (2020)

88. He, K., Zhang, X., Ren, S., Sun, J.: Spatial pyramid pooling in deep convolutional networks for visual recognition. IEEE Trans. Pattern Anal. Mach. Intell. 37(9), 1904–1916 (2015)

89. Lopez, M.M., Ventura, J.: Dilated convolutions for brain tumor segmentation in MRI scans. In: International Conference on Medical Image Computing and Computer-Assisted Intervention (MICCAI) Workshop, pp. 253–262 (2017)

90. Lei, T., Wang, R., Zhang, Y., Wan, Y., Liu, C., Nandi, A.K.: Defed-net: Deformable encoder-decoder network for liver and liver tumor segmentation. IEEE Trans. Radiat. Plasma Med. Sci. (2021)

91. Wang, P., Chen, P., Yuan, Y., Liu, D., Huang, Z., Hou, X., et al.: Understanding convolution for semantic segmentation. Proc. IEEE Winter Conf. Appl. Comput. Vis (WACV), pp. 1451–1460. IEEE, Piscataway, NJ (2018)

92. Yang, L., Song, Q., Wang, Z., Jiang, M.: Parsing r-cnn for instance-level human analysis. Proc. IEEE Conf. Comput. Vis Pattern Recognit (CVPR), pp. 364–373 (2019)

93. Salehi, S.S.M., Erdogmus, D., Gholipour, A.: Tversky loss function for image segmentation using 3d fully convolutional deep networks. Int. Workshop Mach. Learn Med. Imag. 379–387 (2017)

94. Sudre, C.H., Li, W., Vercauteren, T., Ourselin, S., Cardoso, M.J.: Generalised dice overlap as a deep learning loss function for highly unbalanced segmentations. In: Cardoso, M.J., Arbel, T., Carneiro, G., Syeda-Mahmood, T., Tavares, J.M., Moradi, M., Bradley, A., Greenspan, H., Papa, J.P., Madabhushi, A., Nascimento, J.C., Cardoso, J.S., Belagiannis, V., Lu, Z. (eds.) Deep Learning in Medical Image Analysis and Multimodal Learning for Clinical Decision Support. Springer, Berlin, pp. 240–248 (2017)

95. Kervadec, H., Bouchtiba, J., Desrosiers, C., Granger, E., Dolz, J., Ayed, I.B.: Boundary loss for highly unbalanced segmentation. In: Proceedings of The 2nd International Conference on Medical Imaging with Deep Learning (PMLR), pp. 285-296 (2019)

96. Lin, T.Y., Goyal, P., Girshick, R., He, K., Dollár, P.: Focal loss for dense object detection. In: Proceedings of the IEEE International Conference on Computer Vision, pp. 2980–2988 (2017)

97. Wong, K.C., Moradi, M., Tang, H., Syeda Mahmood, T.: 3D segmentation with exponential logarithmic loss for highly unbalanced object sizes. In: Proceedings of the International Conference on Medical Image Computing and Computer-Assisted Intervention, pp. 612–619 (2018)

98. Chen, X., Williams, B.M., Vallabhaneni, S.R., Czanner, G., Williams, R., Zheng, Y.: Learning active contour models for medical image segmentation. In: Proceedings of the IEEE Conference on Computer Vision and Pattern Recognition, pp. 11632–11640. IEEE, Piscataway, NJ (2019)

99. Li, X., Yu, L., Chen, H., Fu, C.W., Xing, L., Heng, P.A., Li Xiaomeng, Yu Lequan, Chen Hao, Fu Chi-Wing, Xing Lei, Heng Pheng-Ann: Transformation-Consistent Self-Ensembling Model for Semisupervised Medical Image Segmentation. IEEE Trans. Neural. Netw. Learn. Syst. 32(2), 523–534 (2021)

100. Karimi, D., Salcudean, S.E.: Reducing the Hausdorff distance in medical image segmentation with convolutional neural networks. IEEE Trans. Med. Imag. 39(2), 499–513 (2020)

101. Taghanaki, S.A., Zheng, Y., Zhou, S.K., Georgescu, B., Sharma, P., Xu, D., et al.: Combo loss: handling input and output imbalance in multi-organ segmentation. Comput. Med. Imag. Graph 75, 24–33 (2019)

102. Caliva, F., Iriondo, C., Martinez, A.M., Majumdar, S., Pedoia, V.: Distance map loss penalty term for semantic segmentation. In: Proceedings of the International Conference on Medical Imaging with Deep Learning–Extended Abstract Track (2019)

103. Dou, Q., Yu, L., Chen, H., Jin, Y., Yang, X., Qin, J., et al.: 3D deeply supervised network for automated segmentation of volumetric medical images. Med. Image Anal. 41, 40–54 (2017)

104. Dou, H., Karimi, D., Rollins, C.K., Ortinau, C.M., Vasung, L., Velasco-Annis, C., Dou Haoran, Karimi Davood, Rollins Caitlin K., Ortinau Cynthia M., Vasung Lana, Velasco-Annis Clemente, Ouaalam Abdelhakim, Yang Xin, Ni Dong, Gholipour Ali: A Deep Attentive Convolutional Neural Network for Automatic Cortical Plate Segmentation in Fetal MRI. IEEE Trans. Med. Imag. 40(4), 1123–1133 (2021)

105. Sirinukunwattana, K., Pluim, J.P., Chen, H., Qi, X., Heng, P.A., Guo, Y.B., et al.: Gland segmentation in colon histology images: The glas challenge contest. Med. Image Anal. 35, 489–502 (2017)

106. Dong, H., Yang, G., Liu, F., Mo, Y., Guo, Y.: Automatic brain tumor detection and segmentation using U-Net based fully convolutional networks. In: Proceedings of the Annual Conference on Medical Image Understanding and Analysis (MIUA), pp. 506–517 (2017)

107. Guibas, J.T., Virdi, T.S., Li, P.S.: Synthetic medical images from dual generative adversarial networks. Preprint, arXiv:170901872 (2017)

108. Mirza, M., Osindero, S.: Conditional generative adversarial nets. Preprint, arXiv:14111784 (2014)

109. Mahapatra, D., Bozorgtabar, B., Thiran, J.P., Reyes, M.: Efficient active learning for image classification and segmentation using a sample selection and conditional generative adversarial network. In: Proceedings of the International Conference on Medical Image Computing and Computer-Assisted Intervention (MICCAI), pp. 580–588 (2018)

110. Shin, H.C., Tenenholtz, N.A., Rogers, J.K., Schwarz, C.G., Senjem, M.L., Gunter, J.L., et al.: Medical image synthesis for data augmentation and anonymization using generative adversarial networks. In: Proceedings of the International Conference on Medical Image Computing and Computer-Assisted Intervention (MICCAI), pp. 1–11 (2018)

111. Jin, D., Xu, Z., Tang, Y., Harrison, A.P., Mollura, D.J.: Ct-realistic lung nodule simulation from 3d conditional generative adversarial networks for robust lung segmentation. In: Proceedings of the International Conference on Medical Image Computing and Computer-Assisted Intervention (MICCAI), pp. 732–740 (2018)

112. Zhu, J.Y., Park, T., Isola, P., Efros, A.A.: Unpaired image-to-image translation using cycle-consistent adversarial networks. In: Proceedings of the IEEE Conference on Computer Vision (ICCV), pp. 2223–2232. IEEE, Piscataway, NJ (2017)

113. Choi, Y., Choi, M., Kim, M., Ha, J.W., Kim, S., Choo, J.: Stargan: unified generative adversarial networks for multi-domain image-to-image translation. In: Proceedings of the IEEE Conference on Computer Vision and Pattern Recognition (CVPR), pp. 8789–8797. IEEE, Piscataway, NJ (2018)

114. Kalinin, A.A., Iglovikov, V.I., Rakhlin, A., Shvets, A.A.: Medical image segmentation using deep neural networks with pre-trained encoders. In: Wani, M., Kantardzic, M., Sayed-Mouchaweh, M. (eds.) Deep Learning Applications, pp. 39–52. Springer, Berlin (2020)

115. Conze, P.H., Brochard, S., Burdin, V., Sheehan, F.T., Pons, C.: Healthy versus pathological learning transferability in shoulder muscle MRI segmentation using deep convolutional encoder-decoders. Comput. Med. Imaging Graph. 83, 101733 (2020)

116. Huo, Y., Xu, Z., Bao, S., Assad, A., Abramson, R.G., Landman, B.A.: Adversarial synthesis learning enables segmentation without target modality ground truth. In: Proceedings of the IEEE 15th International Symposium on Biomedical Imaging (ISBI), pp. 1217–1220. IEEE, Piscataway, NJ (2018)

117. Chen, C., Dou, Q., Chen, H., Qin, J., Heng, P.A.: Synergistic image and feature adaptation: towards cross-modality domain adaptation for medical image segmentation. In: Proceedings of the AAAI Conference on Artificial Intelligence, vol. 33, pp. 865–872 (2019)

118. Chartsias, A., Joyce, T., Dharmakumar, R., Tsaftaris, S.A.: Adversarial image synthesis for unpaired multi-modal cardiac data. In: International Workshop on Simulation and Synthesis in Medical Imaging, pp. 3–13 (2017)

119. Zhao, C., Carass, A., Lee, J., He, Y., Prince, J.L.: Whole brain segmentation and labeling from CT using synthetic MR images. In: International Workshop on Machine Learning in Medical Imaging, pp. 291–298 (2017)

120. Valindria, V.V., Pawlowski, N., Rajchl, M., Lavdas, I., Aboagye, E.O., Rockall, A.G., et al.: Multi-modal learning from unpaired images: Application to multi-organ segmentation in CT and MRI. In: Proceedings of the IEEE Winter Conference on Applications of Computer Vision (WACV), pp. 547–556. IEEE, Piscataway, NJ (2018)

121. Wang, G., Zuluaga, M.A., Li, W., Pratt, R., Patel, P.A., Aertsen, M., et al.: Deepigeos: a deep interactive geodesic framework for medical image segmentation. IEEE Trans. Pattern Anal. Mach. Intell. 41(7), 1559–1572 (2018)

122. Wang, G., Li, W., Zuluaga, M.A., Pratt, R., Patel, P.A., Aertsen, M., et al.: Interactive medical image segmentation using deep learning with image-specific fine tuning. IEEE Trans. Med. Imag. 37(7), 1562–1573 (2018)

123. Boykov, Y.Y., Jolly, M.P.: Interactive graph cuts for optimal boundary & region segmentation of objects in ND images. Proc. IEEE Conf. Comput. Vis. 1, 105–112 (2001)

124. Rother, C., Kolmogorov, V., Blake, A.: "Grabcut" interactive foreground extraction using iterated graph cuts. ACM Trans. Graph 23(3), 309–314 (2004)

125. Rupprecht, C., Laina, I., Navab, N., Hager, G.D., Tombari, F.: Guide me: Interacting with deep networks. In: Proceedings of the International Conference on Medical Image Computing and Computer-Assisted Intervention, pp. 8551–8561 (2018)

126. Zhang, Z., Yang, L., Zheng, Y.: Translating and segmenting multimodal medical volumes with cycle-and shape-consistency generative adversarial network. In: Proceedings of the IEEE Conference on Computer Vision and Pattern Recognition (CVPR), pp. 9242–9251. IEEE, Piscataway, NJ (2018)

127. Baur, C., Albarqouni, S., Navab, N.: Semi-supervised deep learning for fully convolutional networks. In: Proceedings of the International Conference on Medical Image Computing and Comput.-Assist. Intervent., pp. 311–319 (2017)

128. Chartsias, A., Joyce, T., Papanastasiou, G., Semple, S., Williams, M., Newby, D., et al.: Factorised spatial representation learning: Application in semi-supervised myocardial segmentation. Proc. Int. Conf. Med. Image Computing and Computer-Assisted Intervention (MICCAI), pp. 490–498 (2018)

129. Zhao, A., Balakrishnan, G., Durand, F., Guttag, J.V., Dalca, A.V.: Data augmentation using learned transformations for one-shot medical image segmentation. In: Proceedings of the IEEE Conference on Computer Vision and Pattern Recognition, pp. 8543–8553. IEEE, Piscataway, NJ (2019)

130. Elsken, T., Metzen, J.H., Hutter, F.: Neural architecture search: a survey. Preprint, arXiv:180805377 (2018)

131. He, X., Zhao, K., Chu, X.: AutoML: a survey of the state-of-the-art. Knowl.-Based Syst. 212, 106622 (2020)

132. Ha, H., Rana, S., Gupta, S., Nguyen, T., Venkatesh, S., et al.: Bayesian optimization with unknown search space. In: NIPS'19: Proceedings of the 33rd International Conference on Neural Information Processing Systems, pp. 11795–11804 (2019)

133. Vanschoren, J.: Meta-learning: a survey. Preprint, arXiv:181003548 (2018)

134. Chen, L.C., Collins, M., Zhu, Y., Papandreou, G., Zoph, B., Schroff, F., et al.: Searching for efficient multi-scale architectures for dense image prediction. Neural Inform. Process Syst. 31, 8699–8710 (2018)

135. Liu, C., Chen, L.C., Schroff, F., Adam, H., Hua, W., Yuille, A.L., et al.: Auto-deeplab: hierarchical neural architecture search for semantic image segmentation. In: Proceedings of the IEEE Conference on Computer Vision and Pattern Recognition (CVPR), pp. 82–92. IEEE, Piscataway, NJ (2019)

136. Isensee, F., Kohl Simon A. A., Petersen Jens, Maier-Hein Klaus H.: nnU-Net: a self-configuring method for deep learning-based biomedical image segmentation. Nature Methods. 18(2), 203–211 (2021)

137. Weng, Y., Zhou, T., Li, Y., Qiu, X.: Nas-unet: neural architecture search for medical image segmentation. IEEE Access 7, 44247–44257 (2019)

138. Wu, Z., Pan, S., Chen, F., Long, G., Zhang, C., Philip, S.Y.: A comprehensive survey on graph neural networks. IEEE Trans. Neural Netw. Learn. Syst. (2020)

139. Scarselli, F., Gori, M., Tsoi, A.C., Hagenbuchner, M., Monfardini, G.: The graph neural network model. IEEE Trans. Neural Netw. 20(1), 61–80 (2008)

140. Gao, H., Ji, S.: Graph u-nets. Nature (2019)

141. Yang, H., Zhen, X., Chi, Y., Zhang, L., Hua, X.S.: Cpr-gcn: Conditional partial-residual graph convolutional network in automated anatomical labeling of coronary arteries. In: Proceedings of the IEEE/CVF Conference on Computer Vision and Pattern Recognition, pp. 3803–3811. IEEE, Piscataway, NJ (2020)

142. Sun, J., Darbeha, F., Zaidi, M., Wang, B.: Saunet: Shape attentive u-net for interpretable medical image segmentation. Preprint, arXiv:200107645 (2020)

143. Wickstrøm, K., Kampffmeyer, M., Jenssen, R.: Uncertainty and interpretability in convolutional neural networks for semantic segmentation of colorectal polyps. Med. Image Anal. 60, 101619 (2020)

144. Springenberg, J.T., Dosovitskiy, A., Brox, T., Riedmiller, M.: Striving for simplicity: the all convolutional net. Preprint, arXiv:14126806 (2014)

145. Guan, Q., Huang, Y., Zhong, Z., Zheng, Z., Zheng, L., Yang, Y.: Diagnose like a radiologist: attention guided convolutional neural network for thorax disease classification. Preprint, arXiv:180109927 (2018)

146. Tang, Z., Chuang, K.V., DeCarli, C., Jin, L.W., Beckett, L., Keiser, M.J., et al.: Interpretable classification of alzheimer's disease pathologies with a convolutional neural network pipeline. Nat. Commun. 10(1), 1–14 (2019)

147. Selvaraju, R.R., Cogswell, M., Das, A., Vedantam, R., Parikh, D., Batra, D.: Grad-cam: visual explanations from deep networks via gradient-based localization. In: Proceedings of the IEEE Conference on Computer Vision (ICCV), pp. 618–626. IEEE, Piscataway, NJ (2017)

148. Zhang, Z., Chen, P., McGough, M., Xing, F., Wang, C., Bui, M., et al.: Pathologist-level interpretable whole-slide cancer diagnosis with deep learning. Nat. Mach. Intell. 1(5), 236–245 (2019)

149. Dou, Q., Liu, Q., Heng, P.A., Glocker, B.: Unpaired multi-modal segmentation via knowledge distillation. IEEE Trans. Med. Imaging (2020)

150. Hinton, G., Vinyals, O., Dean, J.: Distilling the knowledge in a neural network. Preprint, arXiv:150302531 (2015)

151. Moeskops, P., Wolterink, J.M., van der Velden, B.H., Gilhuijs, K.G., Leiner, T., Viergever, M.A., et al.: Deep learning for multi-task medical image segmentation in multiple modalities. In: Proceedings of the International Conference on Medical Image Computing and Computer-Assisted Intervention (MICCAI), pp. 478–486 (2016)

152. Zhou, T., Ruan, S., Canu, S.: A review: deep learning for medical image segmentation using multi-modality fusion. Array 3, 100004 (2019)

153. Bakas, S., Akbari, H., Sotiras, A., Bilello, M., Rozycki, M., Kirby, J.S., et al.: Advancing the cancer genome atlas glioma MRI collections with expert segmentation labels and radiomic features. Nat. Scient. Data 4, 170117 (2017)

154. Bakas, S., Reyes, M., Jakab, A., Bauer, S., Rempfler, M., Crimi, A., et al.: Identifying the best machine learning algorithms for brain tumor segmentation, progression assessment, and overall survival prediction in the brats challenge. Preprint, arXiv:181102629 (2018)

155. Maier, O., Menze, B.H., von der Gablentz, J., Häni, L., Heinrich, M.P., Liebrand, M., et al.: Isles 2015-a public evaluation benchmark for ischemic stroke lesion segmentation from multispectral MRI. Med. Image Anal. 35, 250–269 (2017)

156. Heller, N., Sathianathen, N., Kalapara, A., Walczak, E., Moore, K., Kaluzniak, H., et al.: The kits19 challenge data: 300 kidney tumor cases with clinical context, CT semantic segmentations, and surgical outcomes. Preprint, arXiv:190400445 (2019)

157. Bilic, P., Christ, P.F., Vorontsov, E., Chlebus, G., Chen, H., Dou, Q., et al.: The liver tumor segmentation benchmark (LITS). Preprint, arXiv:190104056 (2019)

158. Kavur, A.E., Selver, M.A., Dicle, O., Barış, M., Gezer, N.S.: Chaoscombined (CT-MR) healthy abdominal organ segmentation challenge data. Med. Image Anal. 69, 101950 (2019)

159. Smith, K., Clark, W.B.T.N.J.K.M.W.K.: Data from ct_colonography. https://doiorg/107937/K9/TCIA2015NWTESAY1 (2015)

160. Litjens, G., Toth, R., van de Ven, W., Hoeks, C., Kerkstra, S., van Ginneken, B., et al.: Evaluation of prostate segmentation algorithms for MRI: the promise12 challenge. Med. Image Anal. 18(2), 359–373 (2014)

161. Cerrolaza, J.J., Picazo, M.L., Humbert, L., Sato, Y., Rueckert, D., Ballester, M. Á. G., et al.: Computational anatomy for multi-organ analysis in medical imaging: a review. Med. Image Anal. 56, 44–67 (2019)

162. Tan Man, Wu Fa, Kong Dexing, Mao Xiongwei: Automatic liver segmentation using 3D convolutional neural networks with a hybrid loss function. Medical Physics. 48(4), 1707–1719 (2021)

163. France, I.: 3D-IRCADb, 3D image reconstruction for comparison of algorithm database. (2016)

164. Simpson, A.L., Antonelli, M., Bakas, S., Bilello, M., Farahani, K. et al.: A large annotated medical image dataset for the development and evaluation of segmentation algorithms. Preprint, arXiv:190209063 (2019)

165. Kavur, A.E., Gezer, N.S., Barış, M., Conze, P.H., Groza, V., Pham, D.D., et al.: Chaos challenge–combined (CT-MR) healthy abdominal organ segmentation. Preprint, arXiv:200106535 (2020)

166. Roth, H.R., Farag, E.B.T.L.L.J.L.R.M.S.A.: Nih pancreas-ct dataset. http://doiorg/107937/K9/TCIA2016tNB1kqBU (2015)

167. Suinesiaputra, A., Medrano Gracia, P., Cowan, B.R., Young, A.A.: Big heart data: advancing health informatics through data sharing in cardiovascular imaging. IEEE J. Biomed. Health Inform. 19(4), 1283–1290 (2014)

168. Armato, S.G., McLennan, G., Bidaut, L., McNitt-Gray, M.F., Meyer, C.R., Reeves, A.P., et al.: The lung image database consortium (LIDC) and image database resource initiative (IDRI): a completed reference database of lung nodules on CT scans. Med. Phys. 38(2), 915–931 (2011)

169. Topkaya, I.S., Erdogan, H., Porikli, F.: Counting people by clustering person detector outputs. In: 2014 11th IEEE International Conference on Advanced Video and Signal Based Surveillance (AVSS), pp. 313–318. IEEE, Piscataway, NJ (2014)

170. LaMontagne, P.J., Benzinger, T.L., Morris, J.C., Keefe, S., Hornbeck, R., Xiong, C., et al.: Oasis-3: longitudinal neuroimaging, clinical, and cognitive dataset for normal aging and alzheimer disease. medRxiv (2019)

171. Kistler, M., Bonaretti, S., Pfahrer, M., Niklaus, R., Büchler, P.: The virtual skeleton database: an open access repository for biomedical research and collaboration. J. Med. Internet. Res. 15(11), e245 (2013)

172. Codella, N.C., Gutman, D., Celebi, M.E., Helba, B., Marchetti, M.A., Dusza, S.W., et al.: Skin lesion analysis toward melanoma detection: a challenge at the 2017 International Symposium on Biomedical Imaging (ISBI), hosted by the International Skin Imaging Collaboration (ISIC). In: 2018 IEEE 15th International Symposium on Biomedical Imaging (ISBI 2018), pp. 168–172 (2018)

173. Hoover, A., Kouznetsova, V., Goldbaum, M.: Locating blood vessels in retinal images by piecewise threshold probing of a matched filter response. IEEE Trans. Med. Imag. 19(3), 203–210 (2000)

174. Zhang, Y., Lai, H., Yang, W.: Cascade UNet and CH-UNet for thyroid nodule segmentation and benign and malignant classification. In: International Conference on Medical Image Computing and Computer-Assisted Intervention, pp. 129–134. Springer, Berlin (2020)

175. Zhang, B., Xiao, J., Jiao, J., Wei, Y., Zhao, Y.: Affinity attention graph neural network for weakly supervised semantic segmentation. IEEE Trans. Pattern Anal. Mach. Intell. (2021)

176. Yang, B., Pan, H., Yu, J., Han, K., Wang, Y.: Classification of medical images with synergic graph convolutional networks. In: 2019 IEEE 35th International Conference on Data Engineering Workshops (ICDEW), pp. 253–258. IEEE, Piscataway, NJ (2019)

177. Shin, S.Y., Lee, S., Yun, I.D., Lee, K.M.: Deep vessel segmentation by learning graphical connectivity. Med. Image Anal. 58, 101556 (2019)

178. Tian, Z., Li, X., Zheng, Y., Chen, Z., Shi, Z., Liu, L., et al.: Graph-convolutional-network-based interactive prostate segmentation in MR images. Med. Phys. 47(9), 4164–4176 (2020)

179. Dosovitskiy, A., Beyer, L., Kolesnikov, A., Weissenborn, D., Zhai, X., Unterthiner, T. et al.: An image is worth 16x16 words: transformers for image recognition at scale. In: Proceedings of the International Conference on Learning Representations (2019)

180. Chen, J., Lu, Y., Yu, Q., Luo, X., Adeli, E., Wang, Y. et al.: Transunet: transformers make strong encoders for medical image segmentation. Preprint, arXiv:210204306 (2021)

181. Gao, Y., Zhou, M., Metaxas, D.: Utnet: A hybrid transformer architecture for medical image segmentation. In: Proceedings of the International Conference on Medical Image Computing and Computer-Assisted Intervention (MICCAI), pp. 61-71 (2021)

182. Valanarasu, J.M.J., Oza, P., Hacihaliloglu, I., Patel, V.M.: Medical transformer: gated axial-attention for medical image segmentation. Preprint, arXiv:210210662 (2021)

183. Cao, H., Wang, Y., Chen, J., Jiang, D., Zhang, X., Tian, Q. et al.: Swin-unet: Unet-like pure transformer for medical image segmentation. Preprint, arXiv:210505537 (2021)